5-2011

Searching for Melting-Induced Cold-Pool Circulations in an Oklahoma Winter Storm

Gabriel Susca-Lopata
University at Albany, State University of New York

Searching for Melting-Induced Cold-Pool Circulations in an Oklahoma Winter Storm

Gabriel Susca-Lopata

Dept. of Atmospheric and Environmental Sciences

SUNY Albany

Abstract

This paper investigates the thermodynamic and dynamic impacts of melting precipitation through a case study of an Oklahoma winter storm. On 28 January 2005 a rain and snow event affected the state of Oklahoma. A combination of radiosonde data, wind profiler data, radar imagery and Oklahoma Mesonet surface data show that latent cooling from melting caused the surface temperatures to fall in western Oklahoma while evaporation caused surface cooling in central and eastern Oklahoma. The wind and surface pressure fields in western Oklahoma are analyzed along with radar data from Frederick Air Force Base, and some limited evidence for melting-driven downdrafts is found.

1. Introduction

Frozen precipitation melts when it falls into above-freezing air. The ice to liquid phase change takes heat from the environment, so the melting process causes the air to cool where the melting is occurring. Over time, if other processes that would change the temperature are relatively weak; the cooling from melting can create isothermal layer at 0C. In some winter storms, the melting process can cool the air at low levels and allow rain to change over to snow at the surface (Bosart and Sanders 1991; Kain et al. 2000). The cooling effect from melting snow might also modify the mesoscale air-flows within wintertime stratiform precipitation (Atlas et al 1969; Heymsfield 1979; Szeto et al 1988 part II). The present study seeks to determine whether the effects of cooling from melting can create mesoscale density-driven cold-pool circulations in winter storms.

For the purposes of this study the term cold pool has the same meaning as it does with respect to convection. In thunderstorms, negatively-buoyant air cooled by a combination of evaporation and melting (Sanders and Paine, 1975) descends and then spreads out below the storm, forming a dome of relatively cool air, or a ‘cold pool’. Thus a ‘cold pool’ is defined as a mesoscale or convective-scale region of negatively buoyant air that has been cooled by water phase changes. Similarly, the term 'cold pool circulation' used here refers to the combination of the density-driven downdraft, cold outflow and the forced updraft at the edge of a cold pool.

Cold pools from convective storms are associated with high perturbation pressures in the cold pool and low perturbation pressures ahead of and behind the cold pool (Engerer et al. 2008; Wakimoto 1982). Pressure is increased hydrostatically in the cold pool (Wakimoto 1982). Figure 1 shows time series of pressure, equivalent potential temperature, and wind direction from Engerer et al. 2008. The time series were taken at an Oklahoma Mesonet station over a time period in which a mesoscale convective system passed over the station. The pressure at the station begins rising sharply before the passage of the outflow boundary, peaking approximately a half hour after the outflow boundary’s passage. The equivalent potential temperature begins dropping when the outflow boundary arrives, and drops for approximately a half hour following the passage of the outflow boundary. The drop in equivalent potential temperature would correspond to a drop in both temperature and dew point, as is observed in other time series taken during the passage of cold pools (Wakimoto 1982).

Some studies have suggested that melting may play a role in the creation of the cold-pool outflow in convective storms. The model results from Knupp (1988) suggested that melting played an important role in the creation of negative bouyancy in convective downdrafts. Results from a simulation of a mid-latitude mesoscale convective system by Yang and Houze (1995) suggested that melting accounted for roughly a quarter of the strength of the squall-line rear inflow and the mesoscale downdraft.

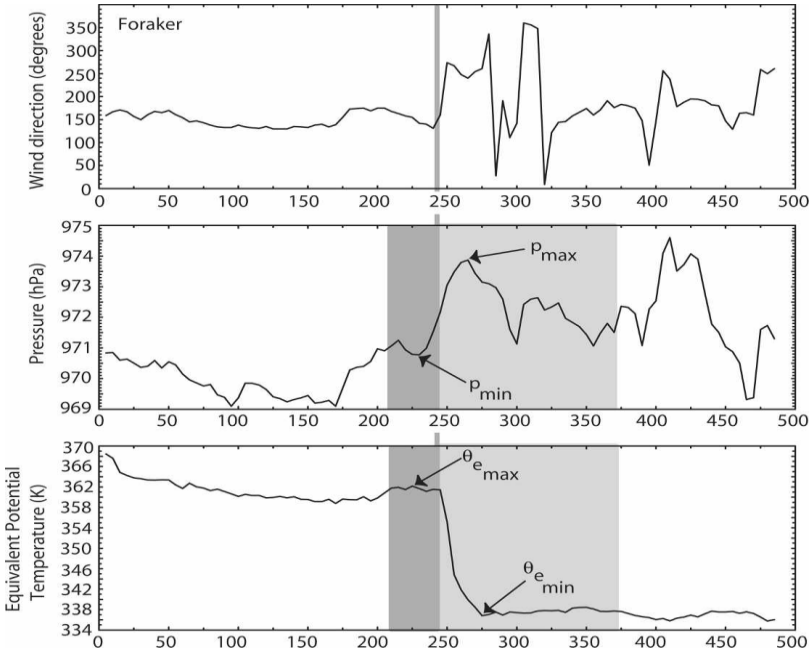

Figure 1. Time Series of pressure (hPa), wind direction, and equivalent potential temperature (Kelvin) at the Foraker, OK mesonet station. Dark shading indicates the 30 minutes prior to the cold pool arrival, light gray shading indicates the two hour period after the cold pool arrival. From Engerer et al. 2008.

Several other authors have provided evidence that the cooling from melting alone can create downdrafts and mesoscale circulations similar to the density-driven circulations observed in convective systems. Atlas et al. (1969) hypothesized that variations in wind near the melting layer in stratiform precipitation could be caused by pressure perturbations due to variations in the rate of melting-induced cooling. Using observations from three radars, Heymsfield (1979) found wind circulations near the surface in an area of precipitation in the warm frontal region of a winter storm, and he attributed the circulations to the cooling from melting snow. Through Doppler radar and wind profiler analysis of a stratiform rainband in a tropical storm, Kim et al (2009) found convergence above the melting layer of the rainband and either relatively weak convergence or positive divergence below the melting layer. Modeling experiments also suggest that the cooling from melting can cause a cold-pool like circulation (Szeto et al 1988 part I and II; Szyrmer and Zawadzki 1999), with downdrafts initiated in the heaviest precipitation.

The purpose of the present study is to find observational evidence of a melting-induced cold pool circulation during a mid-latitude, stratiform precipitation event. To do so, the author needed a conceptual model for possible melting induced circulations, so they would have an idea

of what to look for. However, there are some discrepancies in the results of previous studies on how cold pools in wintertime, stratiform precipitation might behave. The radar observations of a stratiform rainband in a winter storm by Heymsfield (1979) suggest that divergence and therefore positive pressure perturbations would show up underneath the heaviest precipitation. A modeling study by Szyrmer and Zawadzki (1999) also suggests that downdrafts would occur in the heaviest precipitation regions (largest/most intense bright band cores). On the other hand, the modeling work of Szeto et al (1988 part I) suggests that over time the strongest downdrafts propagate away from the precipitation core. Szeto et al. (1988 part II) initialized their model with a horizontal temperature gradient and applied a uniform precipitation rate of 2mm/hr throughout the model domain, with the intention of representing the conditions near a rain-snow line in a winter storm. The authors reported that, by three hours after initialization, the model had an updraft on the snow side of the rain/snow boundary and a downdraft on the rain side, making the circulation thermally indirect.

The possibility of a cold-pool outflow that propagates faster than the core of a precipitation region is considered in the present study. However, the thermally indirect circulation result from Szeto et al (1988 part II) is not considered. Such a circulation would no longer qualify as a cold pool circulation- a negatively buoyant downdraft initiated by diabatic *cooling* must be associated with a thermally direct circulation. The author expects to find evidence of mesoscale downdrafts near where the most melting is happening- near the most intense/deepest bright bands and the sharpest drops in temperature. The author agrees with the reasoning in Szyrmer and Zawadzki (1999): where the most melting occurs, the greatest hydrostatic pressure increases would occur, and the most negative buoyancy would be generated. Specifically, the author expects the following features indicating cold pool outflow: drops in both temperature and dew point coinciding with positive perturbations in pressure and areas of positive wind divergence co-located with the positive pressure perturbations.

The description of the results of this study is divided into several sections. Section 3 provides a synoptic-scale overview of the event studied. Section 4 presents data that show that melting caused cooling occurred near the surface in western Oklahoma and that cooling at lower levels throughout the state may have been caused by melting. Section 5 describes some limited evidence of melting-induced cold pools in western Oklahoma. Section 6 ends the paper with a summary and some concluding remarks.

2. Data and Methodology

First, a large-scale synoptic analysis of the event is performed. For this analysis, Upper Air maps, surface METAR observation maps and radar composites were obtained online from the University Corporation for Atmospheric Research Mesoscale and Microscale Meteorology Division's Image Archive webpage. SKEW-T diagrams and text output of radiosonde data from Norman, OK were obtained online from the University of Wyoming Sounding Page.

Radar, sounding, profiler, and surface station data were used to determine whether melting was the main cause of the observed cooling and changeover from rain to mixed precipitation and snow across Oklahoma. Level II Radar data were obtained from the National Climatic Data Center's Hierarchical Data Storage System, and Level III radar data were viewed using the Oklahoma Climatological Survey's WeatherScope software. Profiler data were taken from the NOAA Profiler Network sites. Oklahoma Mesonet surface station data were used

extensively. The Oklahoma Mesonet network (figure 2) has over 110 surface stations spread across the state of Oklahoma. Data for above-ground variables are available as 5-minute averages (Brock et al 1995). Unfortunately, the mesonet stations do not sense precipitation type. Unlike ASOS stations, the mesonet stations do not have heated tipping buckets, so when frozen precipitation accumulates in the mesonet tipping buckets, the instrument stops reporting precipitation accumulation until the precipitation in the bucket melts (Brock et al 1995 and personal correspondence with OK Climate Survey staff). Therefore, when no accumulated precipitation is reported during a time when precipitation is definitely occurring at a given station (as indicated by radar imagery), one can conclude that frozen precipitation is occurring at said station.

To search for possible cold pool circulations, mesonet wind, pressure, temperature, and dew point data were viewed using the WeatherScope software, and radar data were viewed using both the WeatherScope and GR2Analyst software. The WeatherScope software can display mesonet data either as individual observations from stations or as values that have been interpolated to a grid. Maps of both individual mesonet station observations and gridded data were viewed. An NCAR Command Language script was written to plot surface divergence from the mesonet 10-meter wind data. The script calculates divergence by interpolating mesonet winds to a 0.2X0.2 degree grid and computing the divergence through center finite differencing.

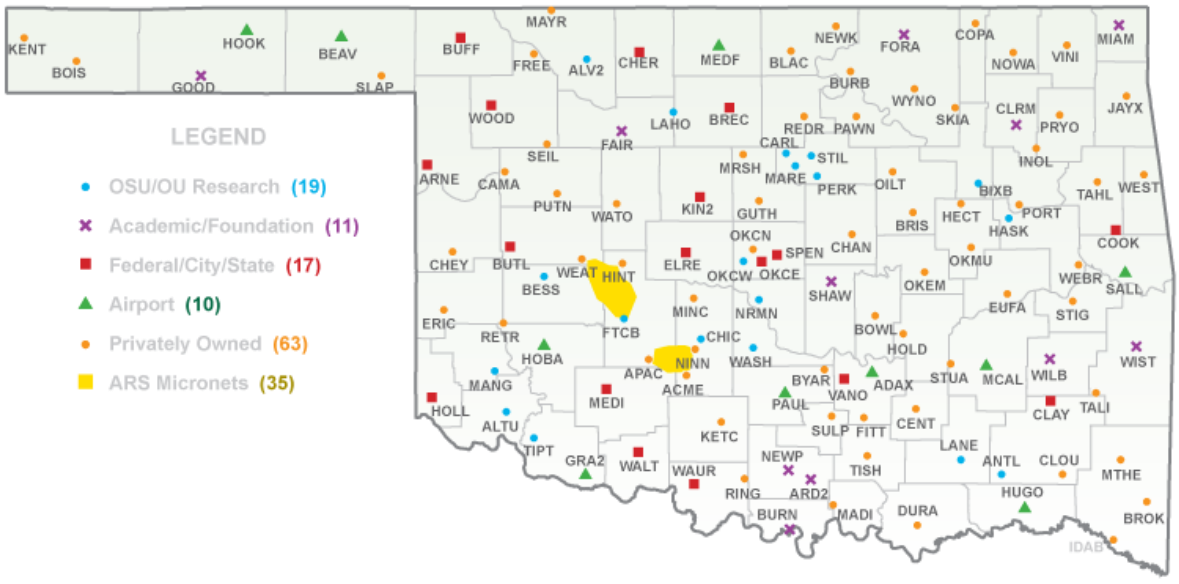

Figure 2. Map of Oklahoma Mesonet sites.

3. Synoptic Overview

Figure 3a shows the 300hPa radiosonde observations and SPC objective analysis at 1200 UTC 28 January. Figures 3b and 3c show 850hPa radiosonde observations and SPC objective analyses at 0000 UTC and 1200 UTC 28 January. Figure 3d shows surface observations and hand-contoured mean sea level pressure at 1200 UTC 28 January. On 27 January 2005 an upper level trough crossed the Rocky Mountains (not shown). An upper-level jet streak also moved across northern Mexico between 0000 UTC and 1200 UTC 28 January (figure 3a). So by 1200 UTC 28 January, the region downstream of the upper level trough was also in the left exit region of the jet streak centered over northern Mexico, enhancing divergence ahead of the upper trough (figure 3a). Between 0000 UTC 28 and 1200 UTC 28 January, a lower-level trough formed east of the Rocky Mountains and spread southward into the southern Plains (figures 3b, c). The associated surface pressure trough can be seen in figure 3d.

Figures 4a through 4d show radar reflectivity composite images for the Southern Plains region at 0000 UTC, 0400 UTC, 0530 UTC and 0800 UTC 28 January respectively. Scattered rain showers affected western OK during the day on 27 January and between 0000 UTC and 0600 UTC 28 January. Between 0400 UTC and 0800 UTC 28 January, a larger area of moderate to heavy precipitation (with a widespread area of reflectivities greater than 25dBZ) filled in across northern Texas ahead of the upper-level trough (figures 4a and 4b). This area of precipitation moved towards western Oklahoma (figure 4c).

Reflectivity composites for the southern Plains at 1100 UTC, 1400 UTC, and 1800 UTC 28 January are displayed in figures 4e through 4g. Between 0800 UTC and 1600 UTC, the area of moderate to heavy precipitation overspread western and central OK from west to east. Most locations in Oklahoma experienced 3-6 hours of moderate to heavy precipitation, with a longer duration of continuous precipitation in northwest OK. Temperatures fell during the period of moderate to heavy precipitation, and rain changed to snow through most of Oklahoma. For example, between 1300 UTC and 1500 UTC, precipitation type changed from rain to sleet and then to heavy snow in Oklahoma City.

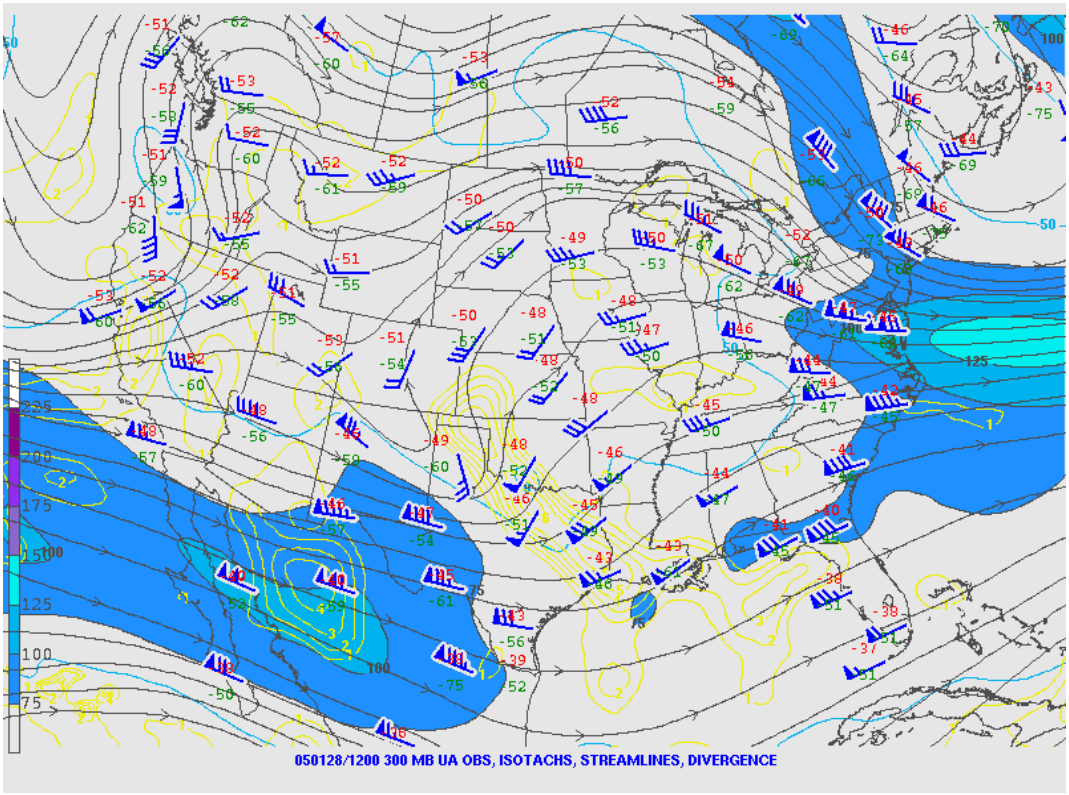

Figure 3a. 300hPa temperature, dew point and winds from radiosonde observations and 300 hPa streamlines and divergence (yellow contours) from SPC objective analysis at 1200 UTC 28 January 2005.

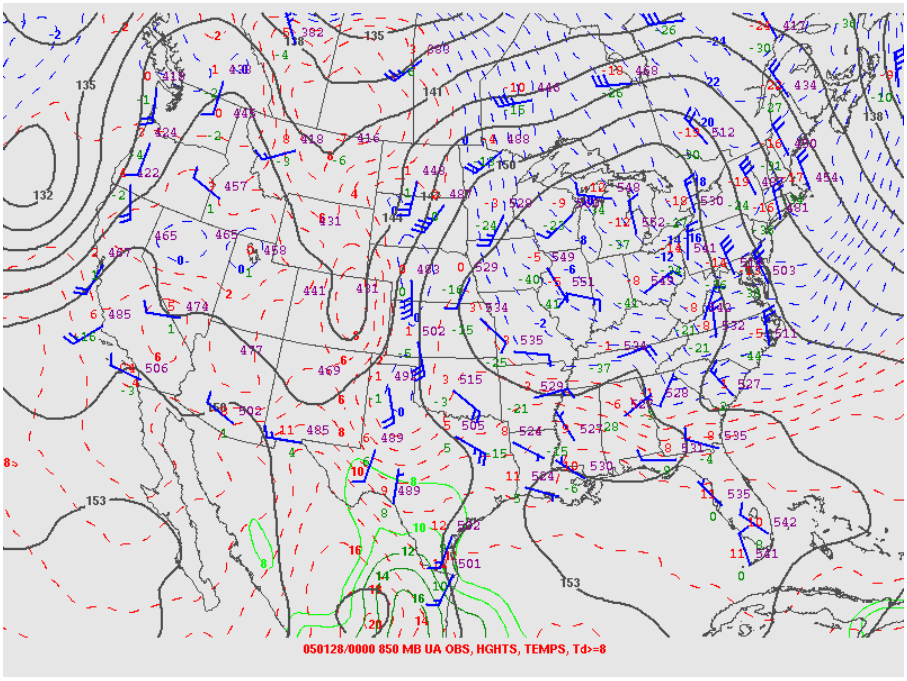

Figure 3b. 850hPa temperature, dew point and winds from radiosonde observations at 0000 UTC 28 January 2005. 850hPa geopotential height (solid black contours, decameters), temperature (dashed contours, degC) and dew points greater than 8degC (solid green contours) from SPC objective analysis at 0000 UTC 28 January 2005.

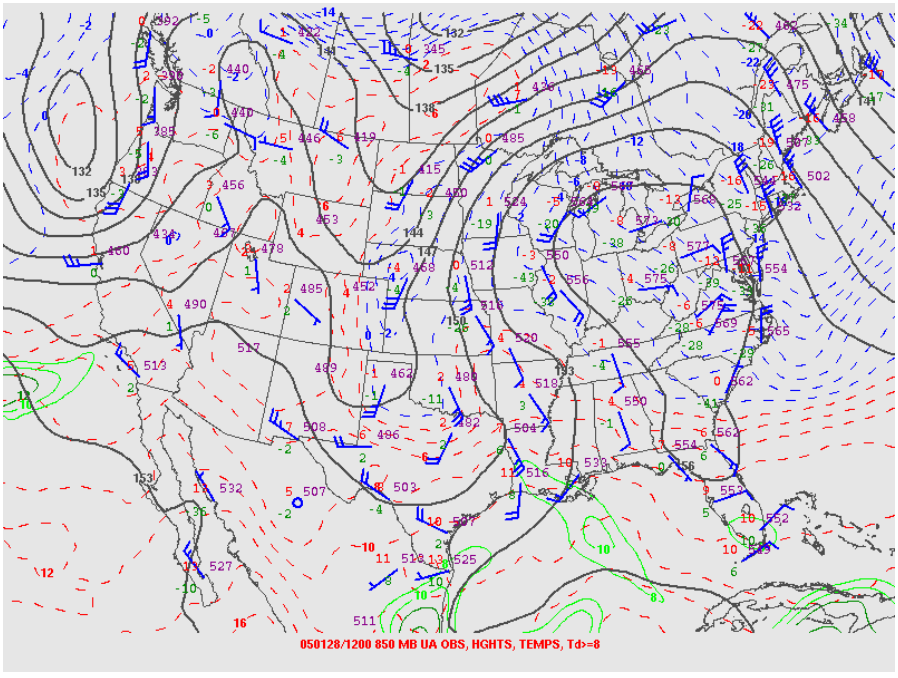

Figure 3c. As in figure 3b, but for 1200 UTC 28 January 2005.

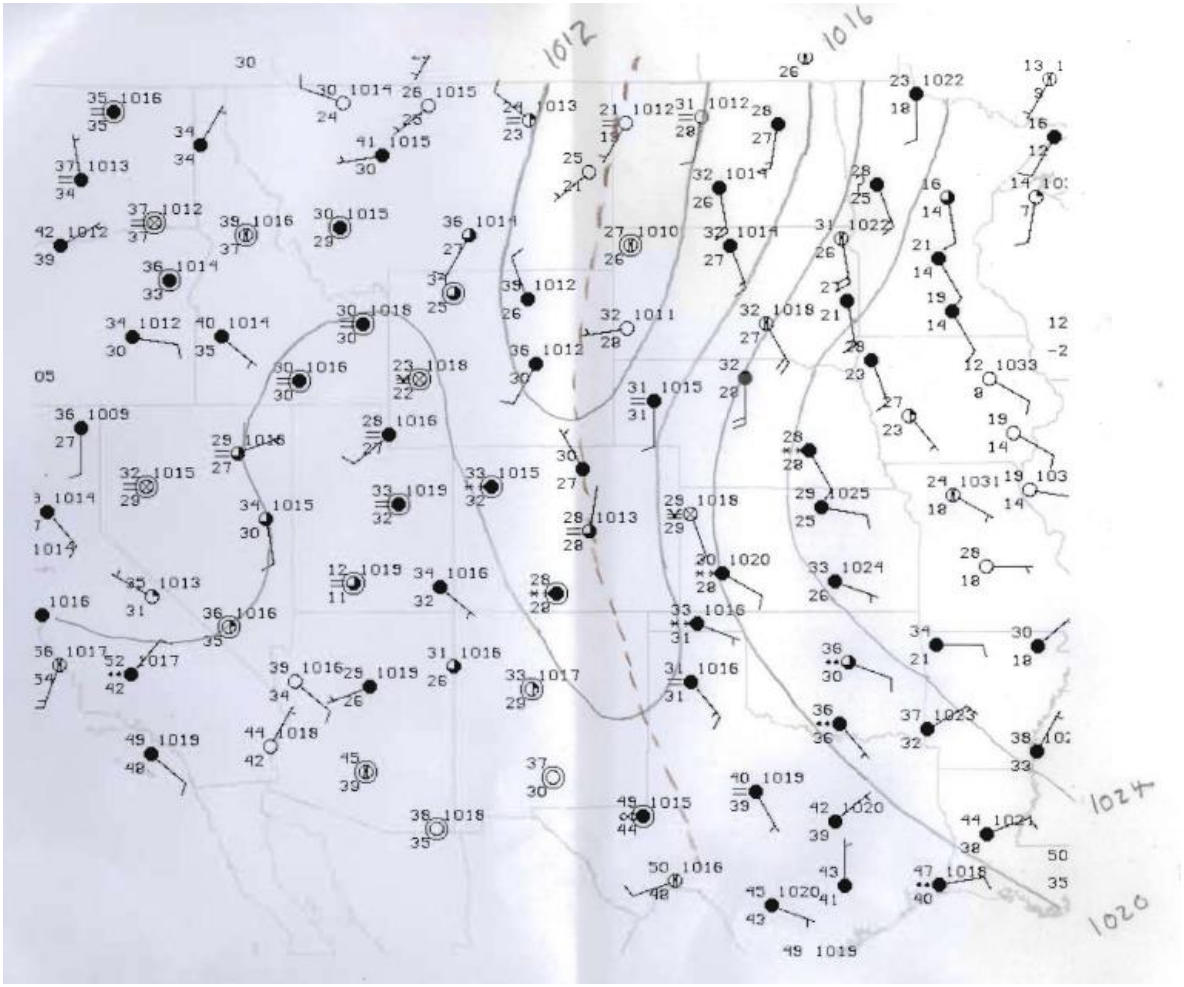

Figure 3d. Surface observations of temperature and dew point (degC), pressure (hPa) and wind (knots), and hand-contoured pressure (hPa) at 1200 UTC 28 January 2005. The brown dashed line indicates the axis of the surface trough.

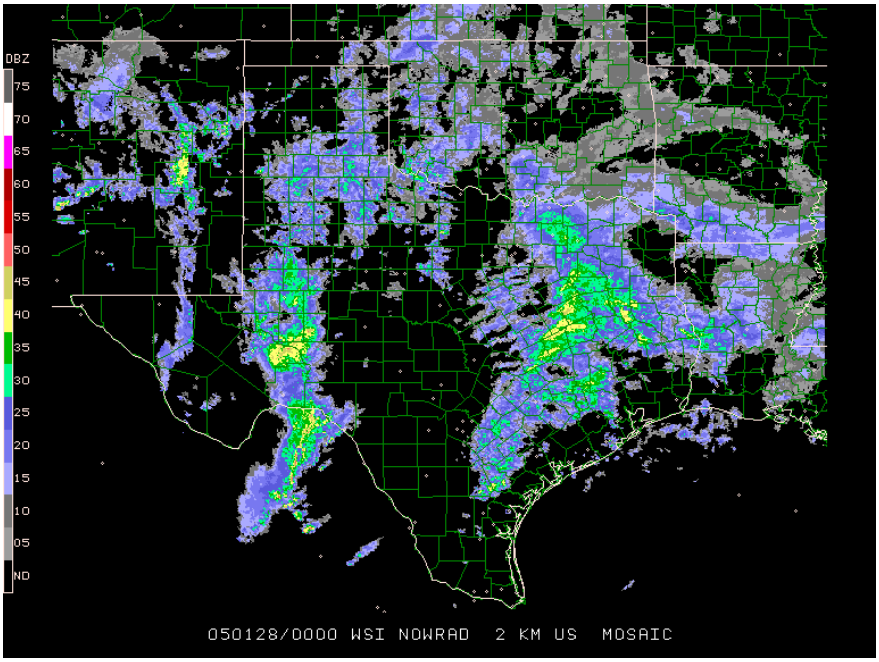

Figure 4a. WSI Southern Plains reflectivity composite image at 0000Z 28 January 2005.

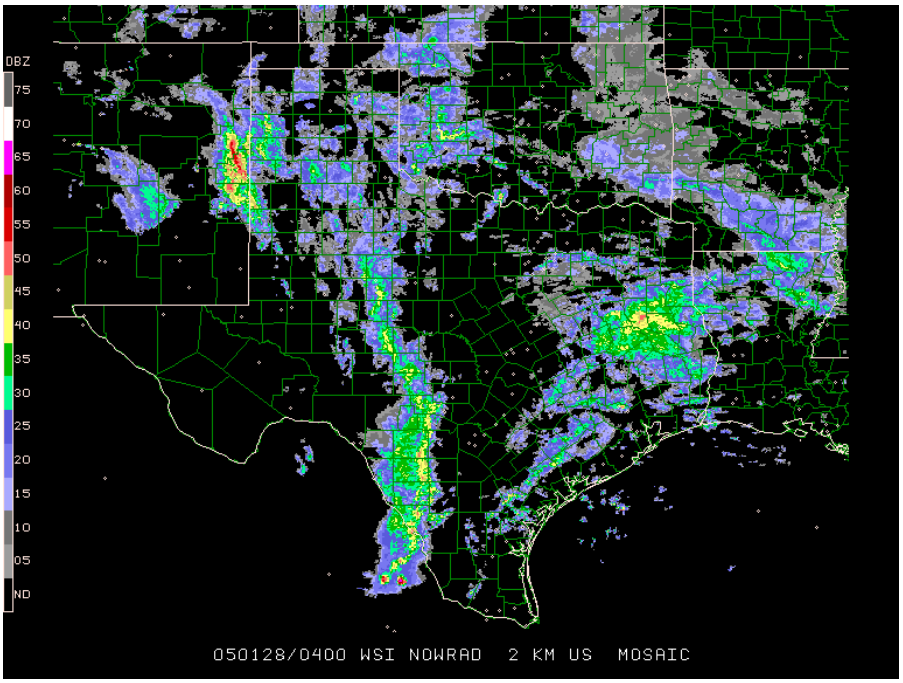

Figure 4b. WSI Southern Plains reflectivity composite image at 0400 UTC 28 January 2005.

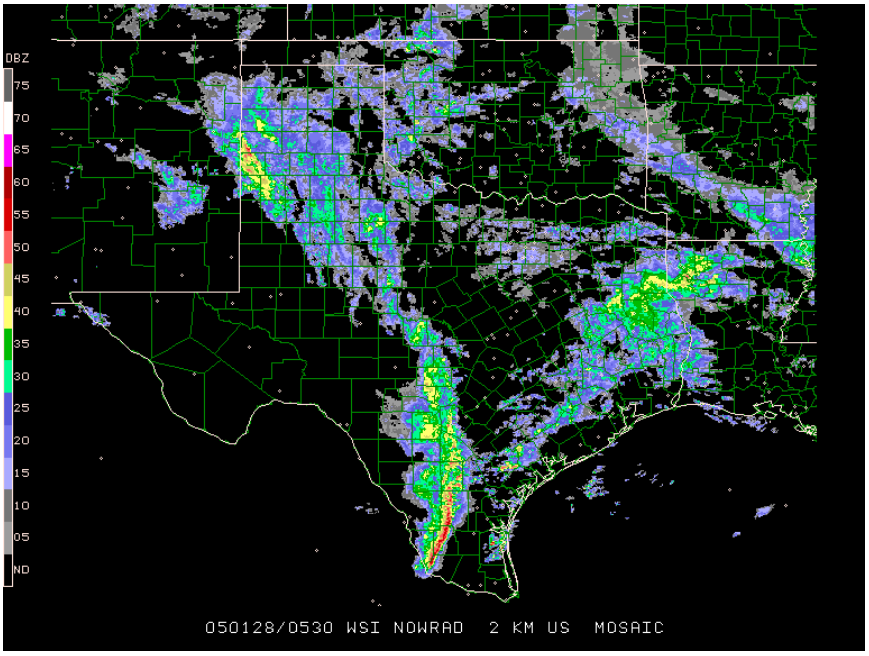

Figure 4c. WSI Southern Plains reflectivity composite image at 0530 UTC 28 January 2005.

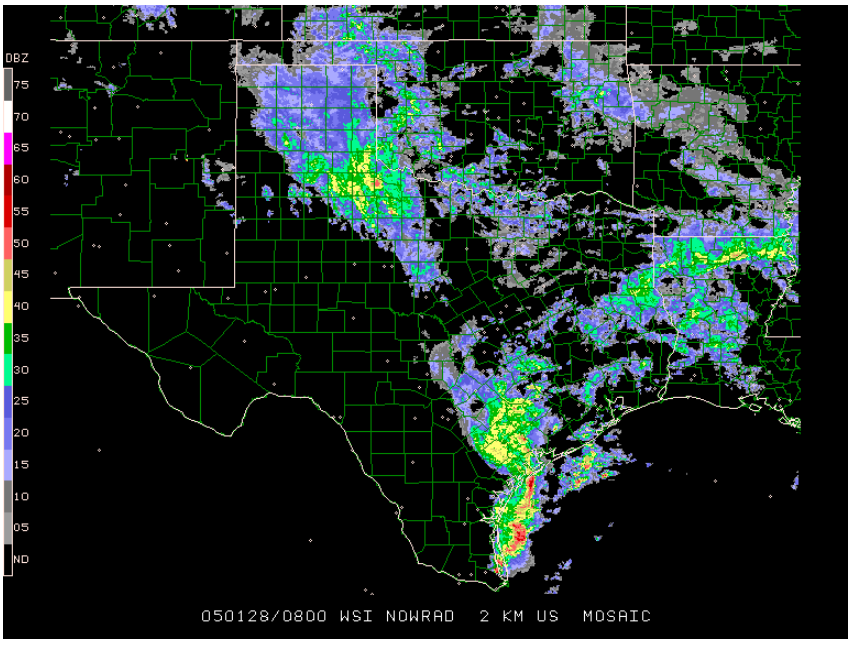

Figure 4d. WSI Southern Plains reflectivity composite image at 0800 UTC 28 January 2005.

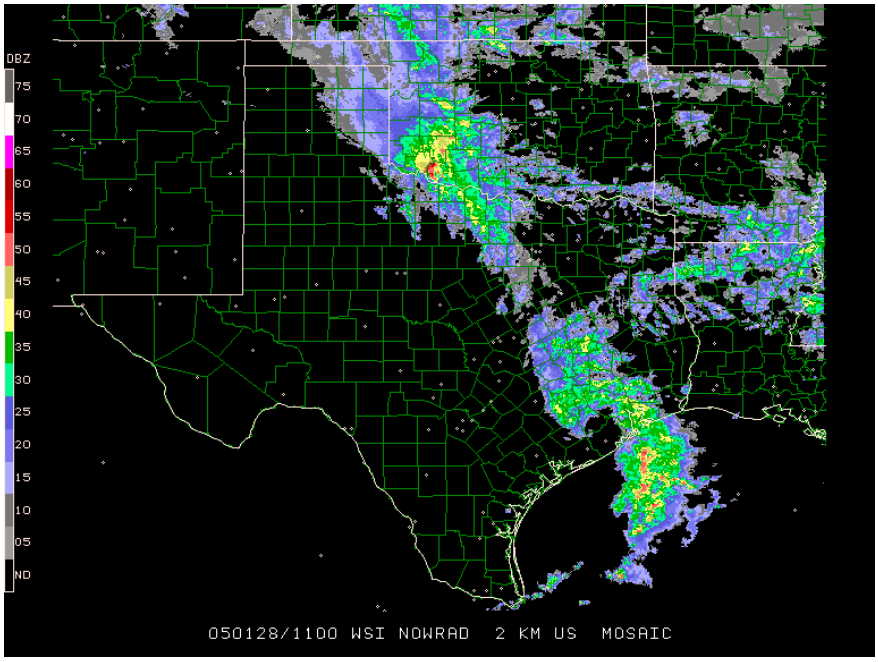

Figure 4e. WSI Southern Plains reflectivity composite image at 1100 UTC 28 January 2005.

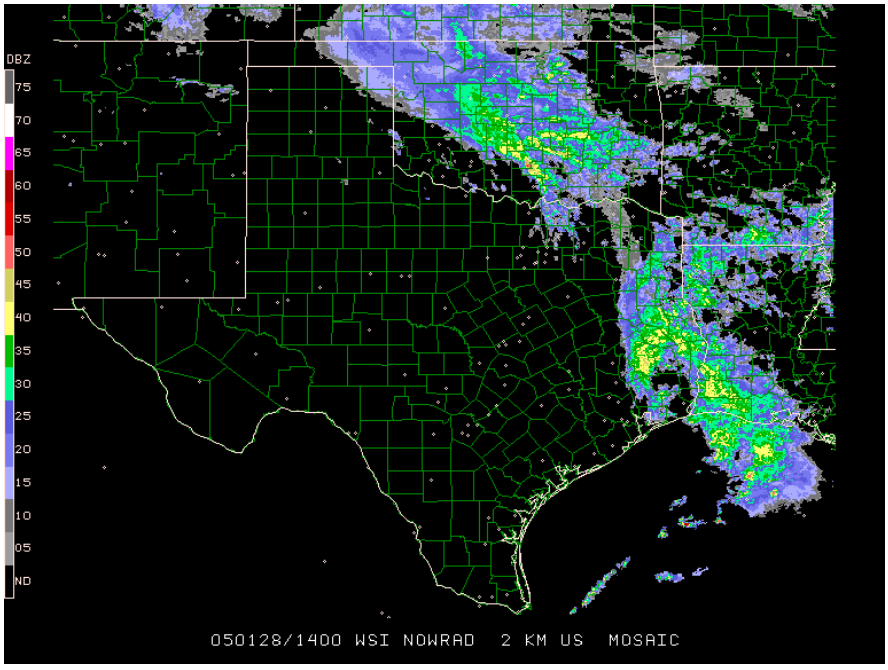

Figure 4f. WSI Southern Plains reflectivity composite image at 1400 UTC 28 January 2005.

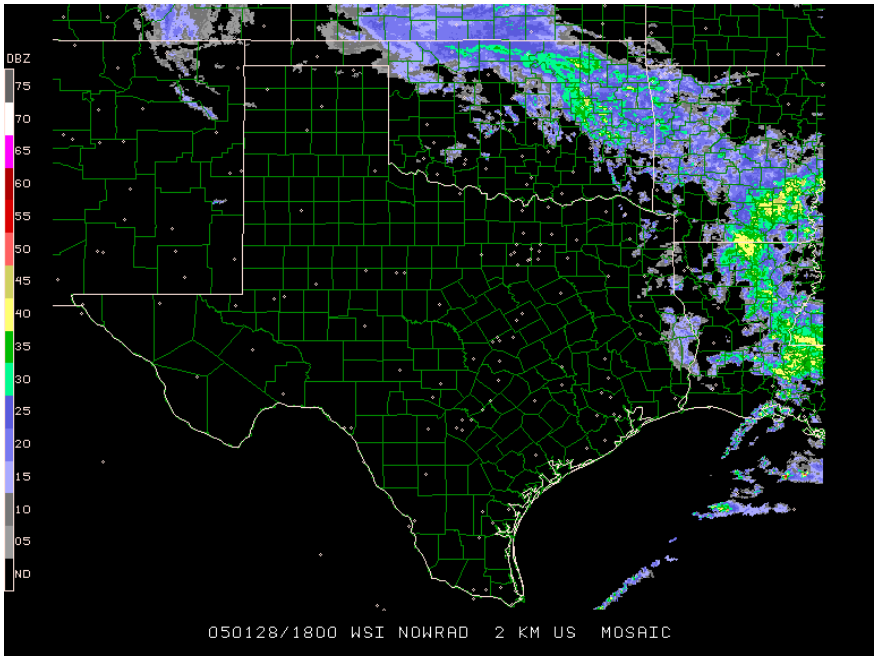

Figure 4g. WSI Southern Plains reflectivity composite image at 1800 UTC 28 January 2005.

4. Cooling due to Melting.

The processes that can contribute to local cooling are described by the thermodynamic energy equation:

$$\frac{\partial T}{\partial t} + \vec{V}_h \cdot \nabla T - S_p \omega = \frac{\dot{Q}}{c_p}$$

A B C D

Term A is the temperature tendency at a point. Term B is horizontal temperature advection. Term C accounts for vertical temperature advection and adiabatic expansion or compression. Term D is the diabatic heating term, accounting for processes including radiative heating, evaporation, and melting. To be able to conclude that melting dominated the atmospheric cooling, other processes

that cause temperature changes must be either relatively weak or act to warm the atmosphere. Since the changeovers from rain to snow occurred during the daytime hours in Oklahoma, radiative cooling can be ruled out immediately. Observations are presented in this section to assess the temperature tendencies in Oklahoma due to advection and evaporative cooling.

Cooling due to vertical advection, or "layer lifting", cannot be ruled out from looking at the sounding and surface data. The moderate to heavy precipitation was occurring in an area of upper-level divergence (figures 3a and the 4e-4g), and the presence of a large area of precipitation implies large scale ascent, so some cooling due to 'layer lifting' was likely occurring. However, quantifying the cooling due to synoptic scale ascent would require vertically integrating horizontal divergence, which is beyond the scope of this paper.

Figures 5 is a SKEW-T diagram of sounding data from Norman, Oklahoma (OUN) at 1200 UTC 28 January. A time-height cross-section of winds from the Purcell, Oklahoma profiler is shown in figure 6. The temperatures in the 1200 UTC OUN sounding are above freezing both near the surface and between approximately 850mb and 750mb (figure 5). The maximum temperature in 750mb-850mb warm nose is 3.6C, and the temperature at 978mb is 2.6C. With a maximum temperature in the warm layer greater than 3C and a 978mb temperature of nearly 3C, snow could not have fallen at OUN unless the 850mb-750mb warm layer was cooled (Baumgardt, 1999), and it is unlikely that any snow reached the surface without the near-surface air also being cooled. The winds in the OUN sounding veer from southeast to southwest between the surface and 500hPa, indicating warm advection. Veering low-level profiler winds indicate that warm advection occurred at low levels for the duration of the moderate to heavy precipitation, and backing mid-level winds after 1500 UTC indicate that cold advection occurred above 700mb just when the precipitation was ending (figures 6 and 7e). Recall from figures 3b and 3c that the 850hPa height contours and rawinsonde observations imply warm advection everywhere in Oklahoma except the Oklahoma Panhandle at 00Z 28 January, and warm advection through central and western Oklahoma at 1200 UTC 28 January. Where the geostrophic temperature advection does not appear to be positive in figures 3b and 3c, it is nearly neutral. Therefore, it is highly unlikely that horizontal temperature advection caused the observed cooling that occurred in Oklahoma.

If cooling was not caused by horizontal advection or vertical motion, then the cooling must have been due to diabatic effects. When the atmosphere is not saturated, evaporation of rain and sublimation of snow dominate the diabatic cooling, since the latent heat of vaporization is approximately an order of magnitude greater than the latent heat of melting. There is an unsaturated layer in the 1200 UTC OUN sounding near 850mb. If large scale ascent were to lift this dry layer, evaporation could cool the warm nose. However, the dry layer in the OUN sounding might not be representative of the conditions throughout Oklahoma. The scattered showers that occurred between 0000 UTC 28 January and 0600 UTC 28 January across western Oklahoma probably saturated the profile there. The cooling from melting precipitation may have been solely responsible for eliminating the 750mb-850mb warm nose in western Oklahoma, and partly responsible for cooling the 750-850mb warm nose in other portions of Oklahoma.

Figures 7a through 7d show maps of mesonet temperature, dew point and wind observations, and radar reflectivity from Frederick Air Force Base (KFDR) at 7000 UTC, 9000 UTC, 1100 UTC and 1300 UTC 28 January. Figures 7d through 7g display the same data from 1500 UTC to 19 UTC, except the base reflectivity is from Oklahoma City (KTLX). In figure 7a, there is some scattered rainfall in parts of Oklahoma, but the moderate to heavy precipitation has

not entered the state yet. Note that the dew points are above freezing and very close to the temperatures in western Oklahoma, while the dew points are further from the temperatures and below freezing in central and eastern Oklahoma. Figures 7a through 7d illustrate the cooling at the surface as the moderate to heavy precipitation (widespread area of greater than 25dBZ reflectivity) moved through Oklahoma. In western Oklahoma, both the temperature and dew point fell during the moderate to heavy precipitation. In central and eastern Oklahoma, the temperatures fell while the dew points rose. Because the surface air was saturated in western Oklahoma and low-level warm advection prevailed throughout the state while the precipitation fell, temperatures and dew points falling simultaneously indicate that melting caused the surface cooling in western Oklahoma. The sub-saturated conditions and rising dew points across central and eastern Oklahoma indicate that evaporation caused the surface cooling in those portions of the state.

Time series from several stations in Oklahoma further illustrate that melting caused the surface cooling in western Oklahoma, while evaporation caused the surface cooling in central and eastern Oklahoma. Figures 8a through 8f display time series of temperature, dew point, pressure and accumulated rainfall at the following respective stations: Hollis (HOLL), Altus (ALTU), Tipton (TIPT), Mangum (MANG), Okema (OKEM), and Oilton (OILT). At HOLL, ALTU, TIPT, and MANG (figure 8a through 8d), the dew point and temperature are nearly equal before the temperature begins to drop sharply. During the moderate to heavy precipitation, the dew point and temperature fall together at these stations, and saturation is maintained. At OKEM and OILT (figures 8e and 8f), the temperature and dew point are initially far apart, and then the temperatures fall while the dew points rise, then the dew points and temperatures remain nearly constant at OILT and rise slightly at OKEM.

A combination of observations show that warm advection was occurring during the moderate to heavy precipitation, the surface air was saturated in western Oklahoma, and the air up through the 850-750mb warm layer was possibly also saturated. This means that the surface cooling that happened in western Oklahoma during the period of moderate to heavy precipitation must have been caused by melting, and the low level cooling was possibly also caused by melting. The next section will focus on western Oklahoma and will present some evidence of the existence of cold pool circulations due to melting.

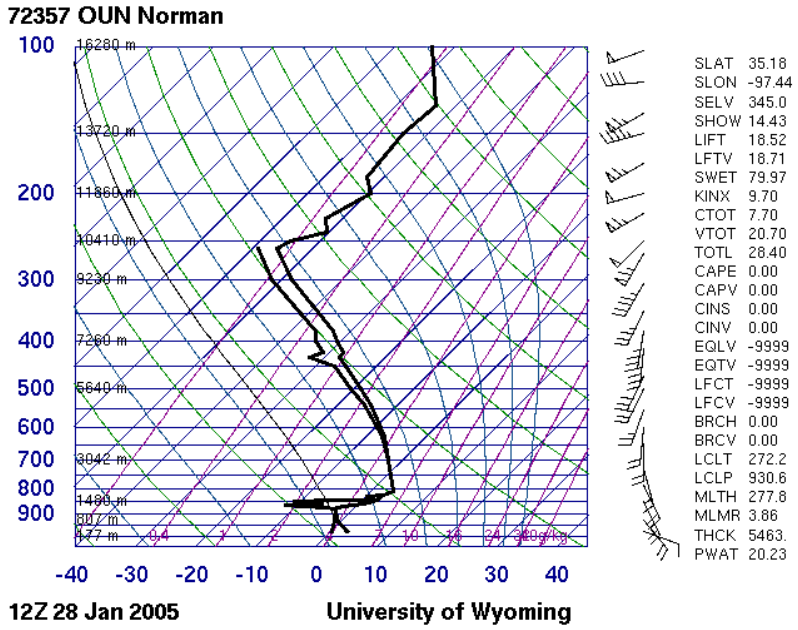

Figure 5. SKEW-T/logP diagram of OUN sounding data from 12 UTC 28 January.

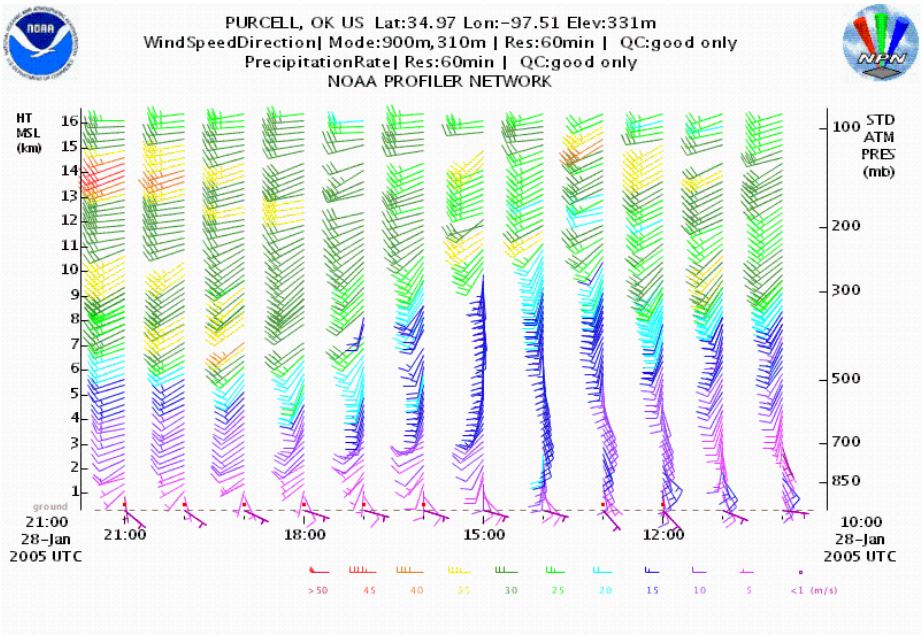

Figure 6. Time-height cross-section of winds (knots) from the Purcell, Oklahoma profiler. Time (UTC) from right to left beginning at 1000 UTC 28 January 2005 and ending at 2100 UTC 28 January 2005.

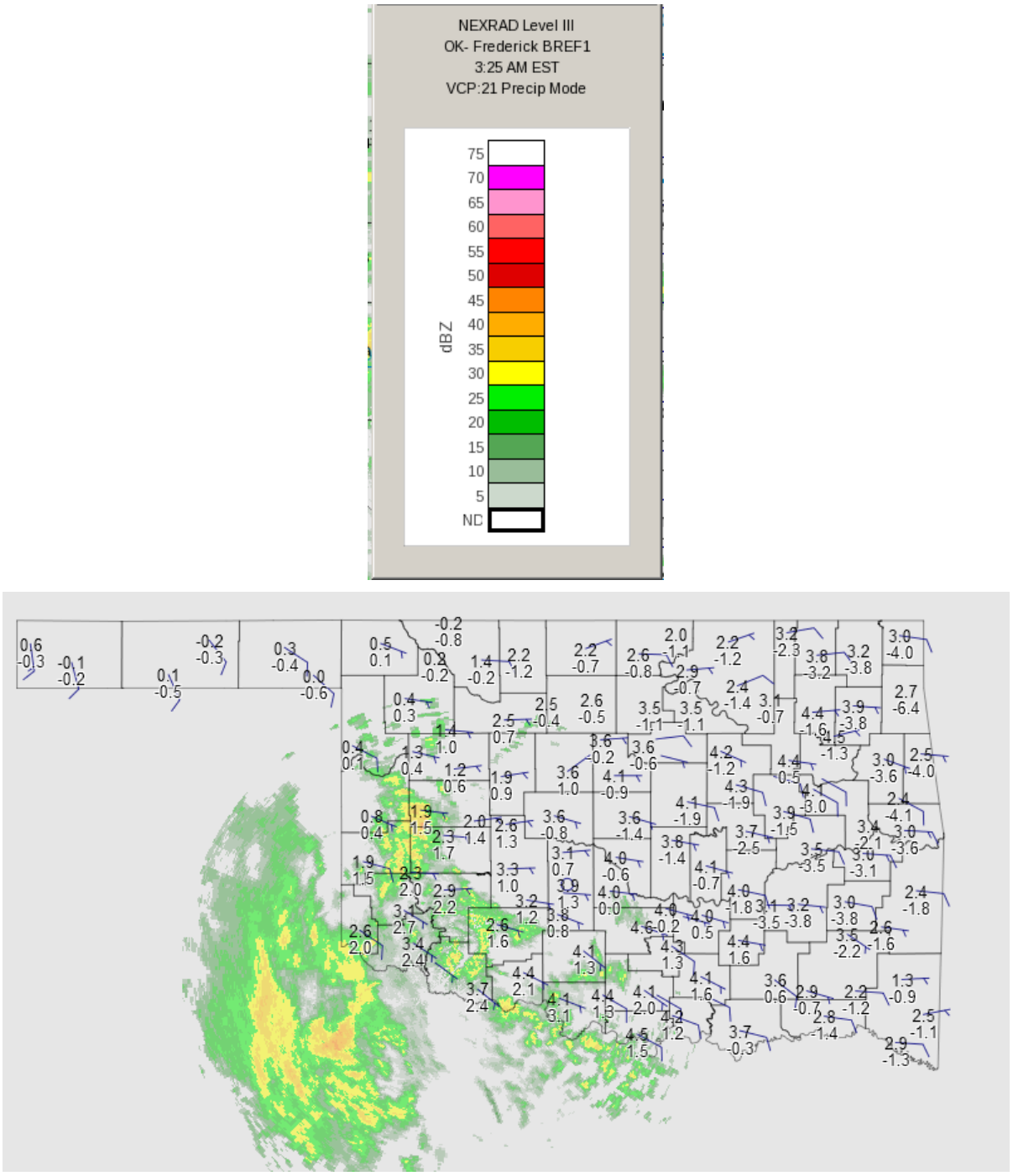

Figure 7a. Mesonet temperature (black text), dew point (outlined black text underneath temperature), and wind observations (barbs) at 0700 UTC 28 January. Temperature and dew point are in degrees Celcsius, winds are in knots. A colorbar for the radar reflectivities is above the figure.

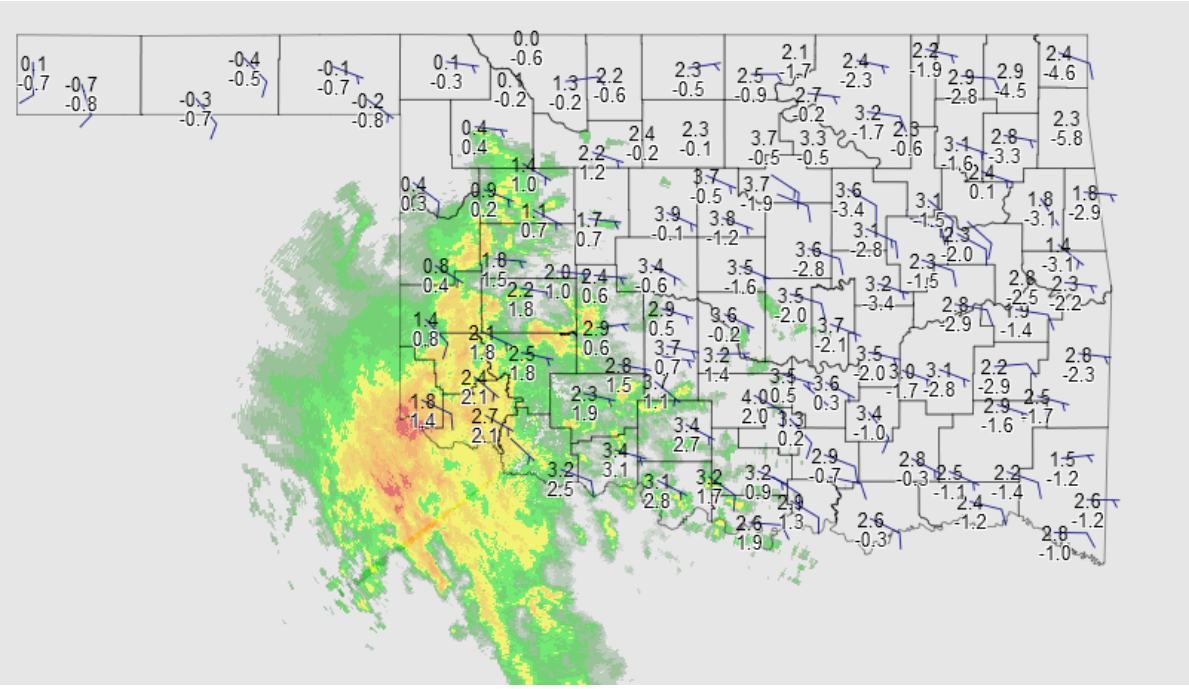

Figure 7b. As in 7a, but at 0900 UTC 28 January.

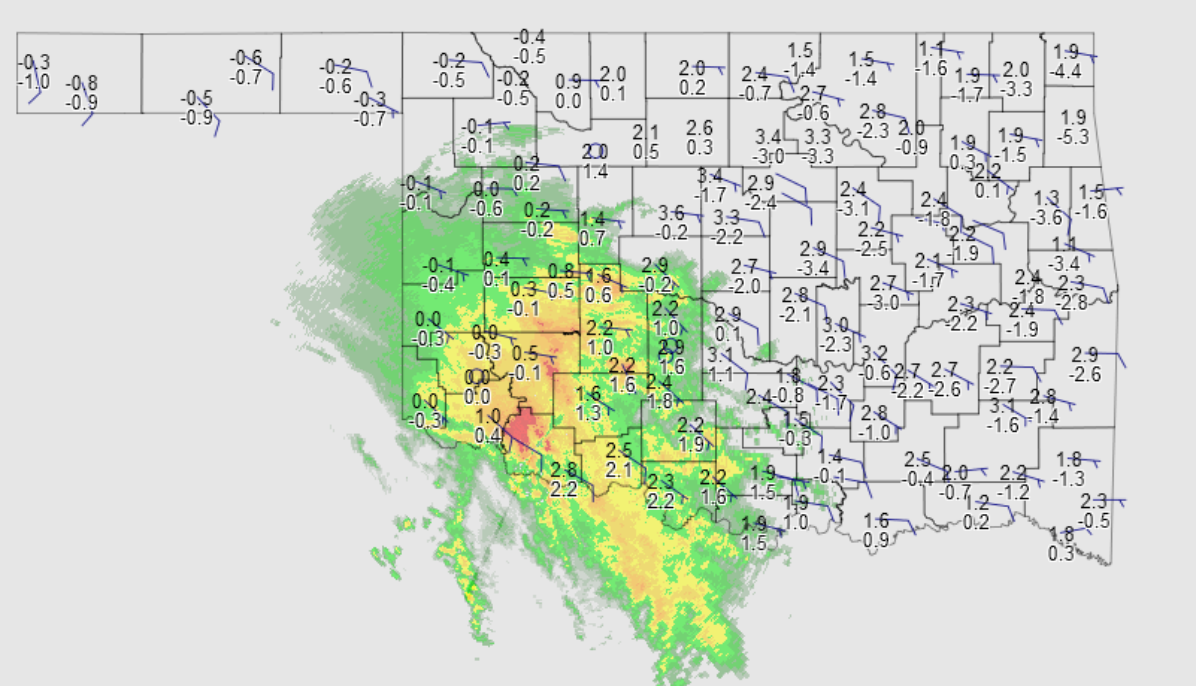

Figure 7c. As in 7a, but at 1100 UTC 28 January.

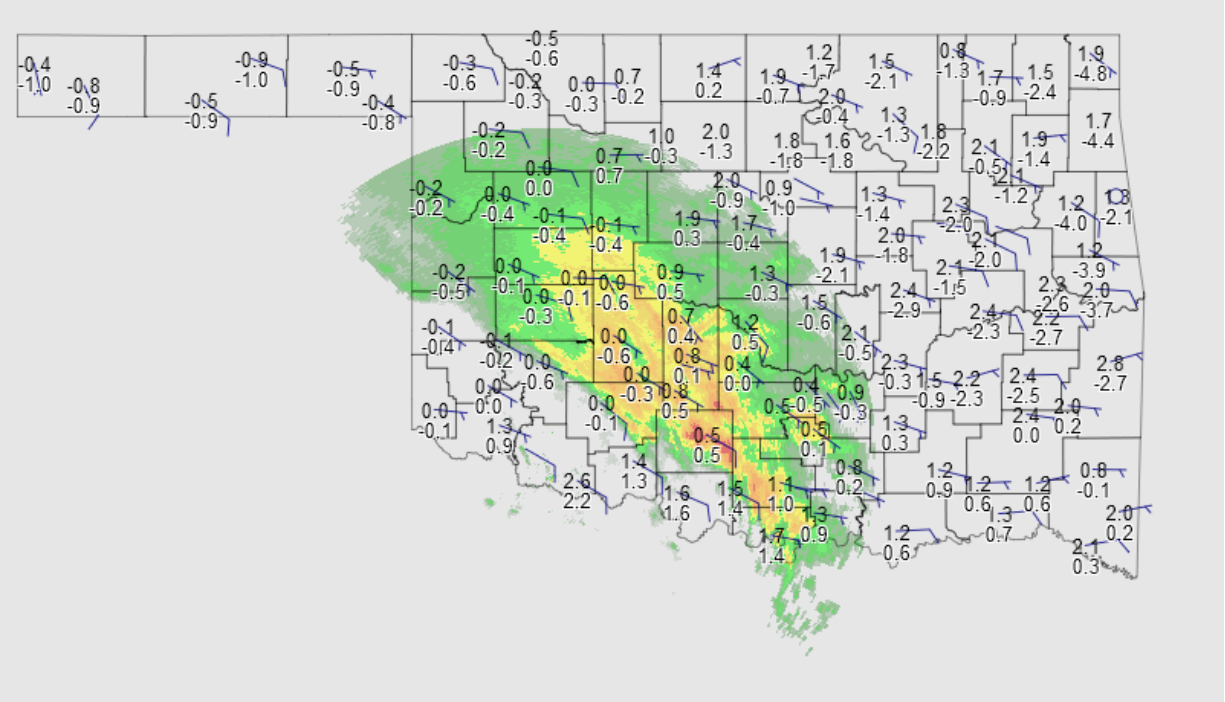

Figure 7d. As in 7a, but at 1300UTC 28 January.

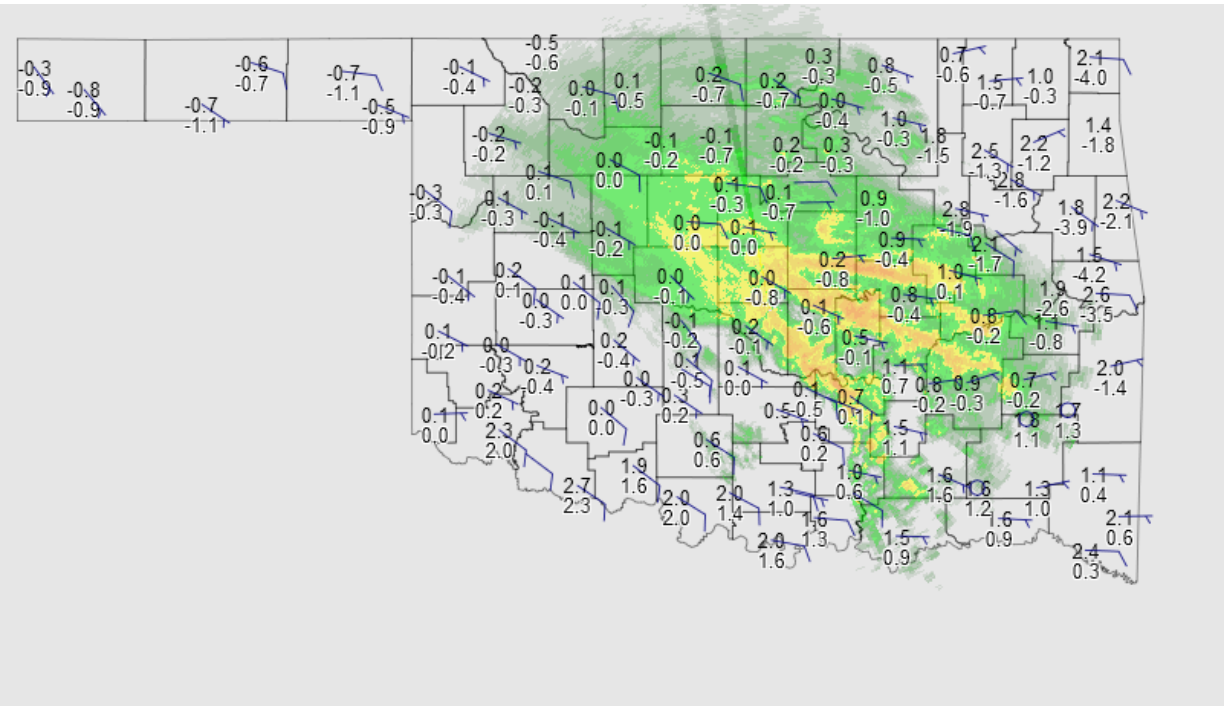

Figure 7e. As in 7a, but at 1500 UTC 28 January.

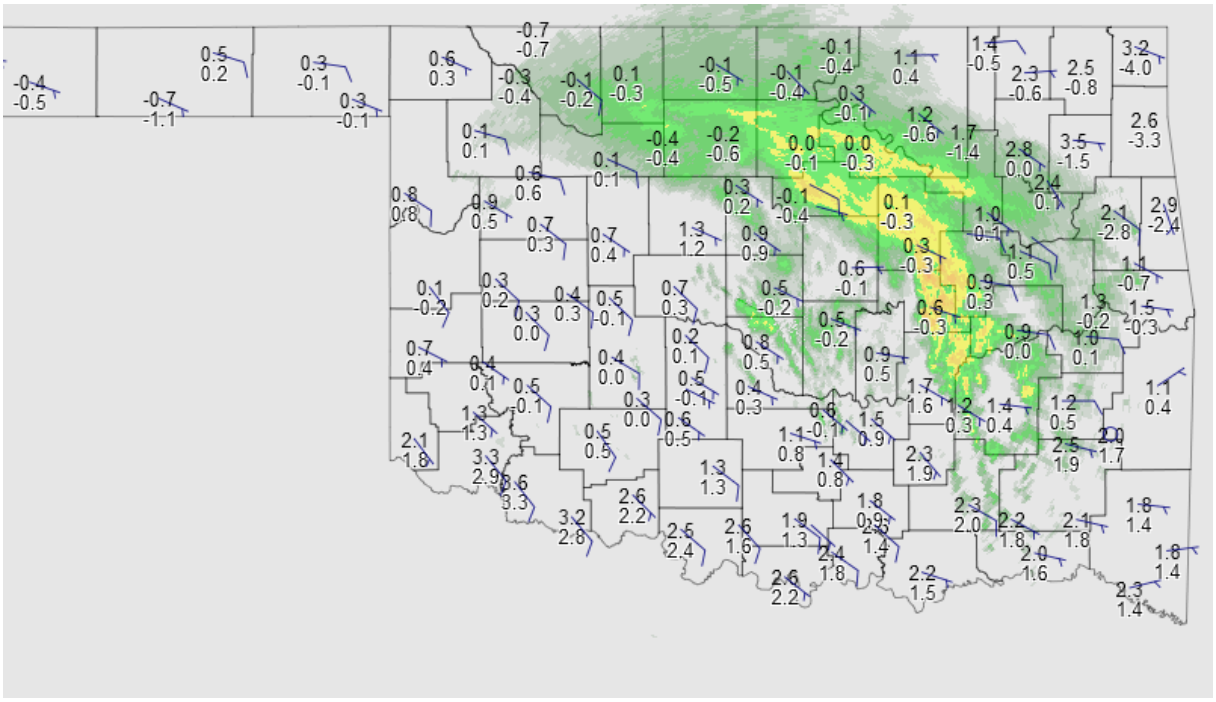

Figure 7f. As in 7a, but at 1700 UTC 28 January.

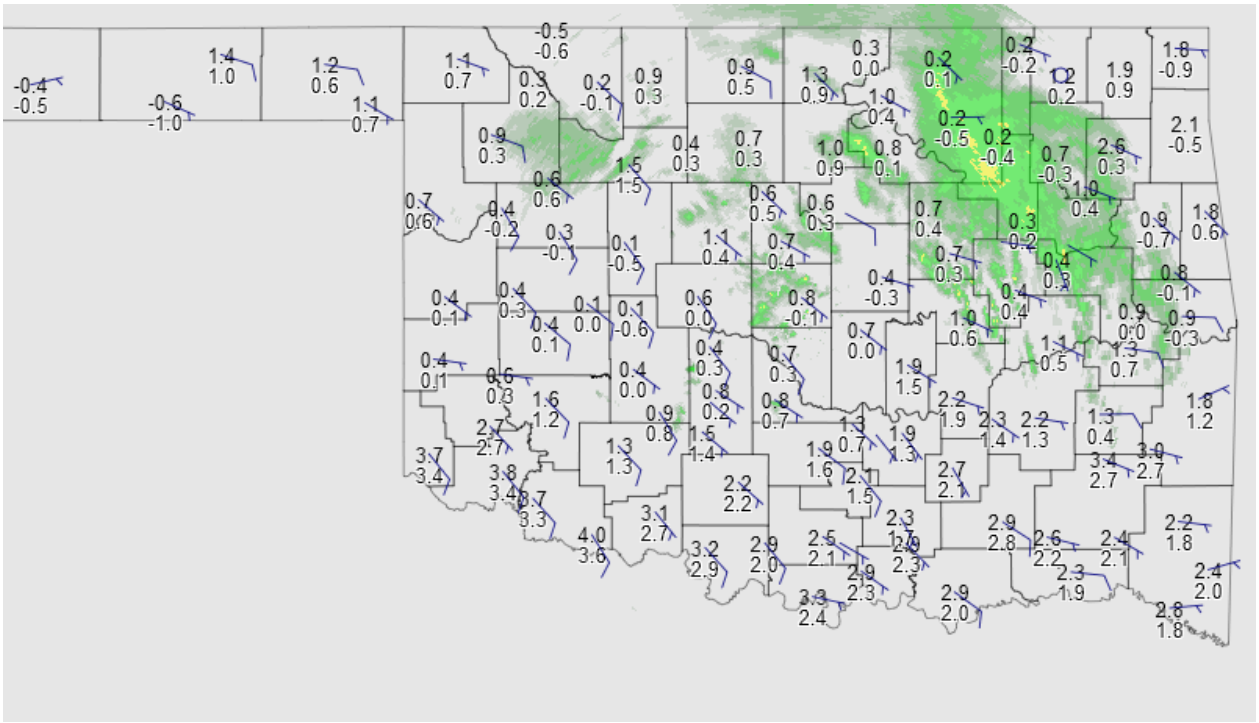

Figure 7g. As in 7a, but at 1900 UTC 28 January.

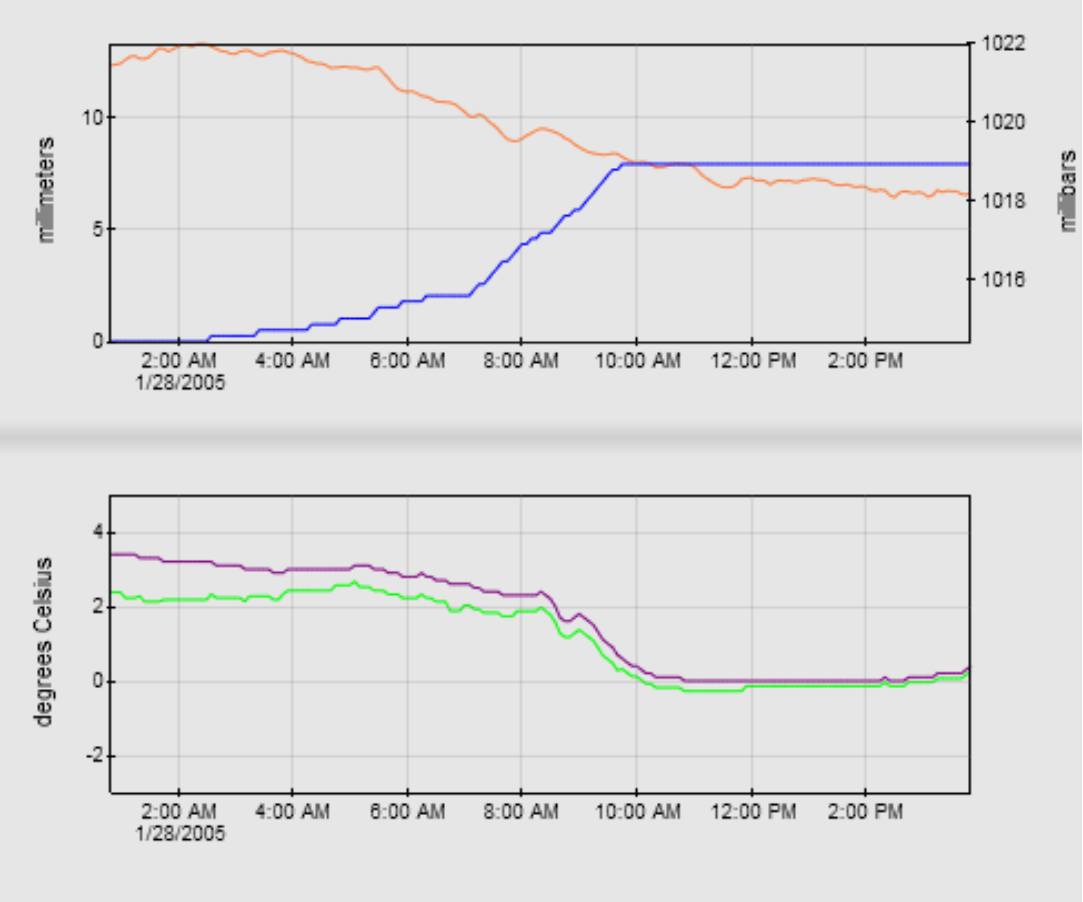

Figure 8a. Time series at Hollis, OK. Pressure (mb) and accumulated rainfall (mm) are in the top panel, dew point and temperature (degC) are in the bottom panel. Time (GMT) along the bottom axis.

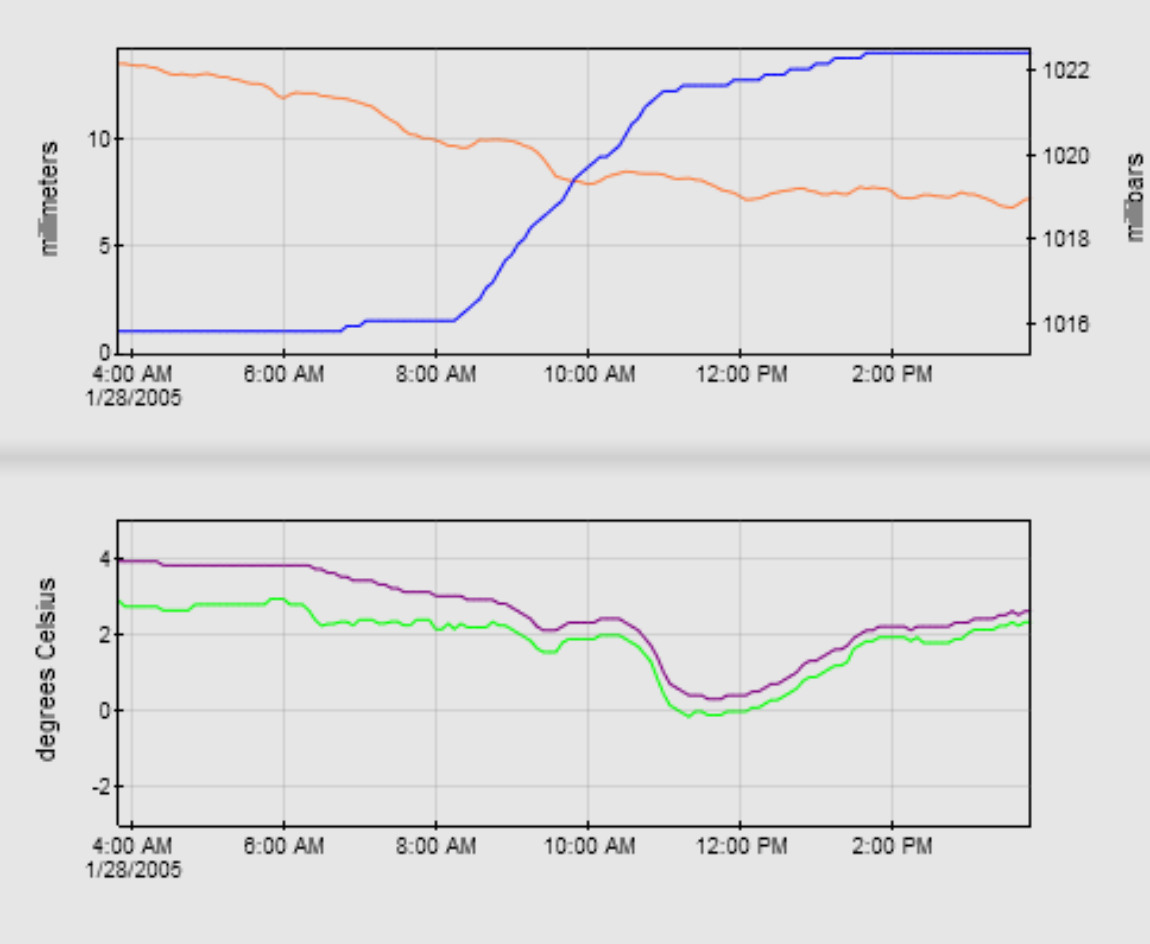

Figure 8b. As in 8a, but at ALTU.

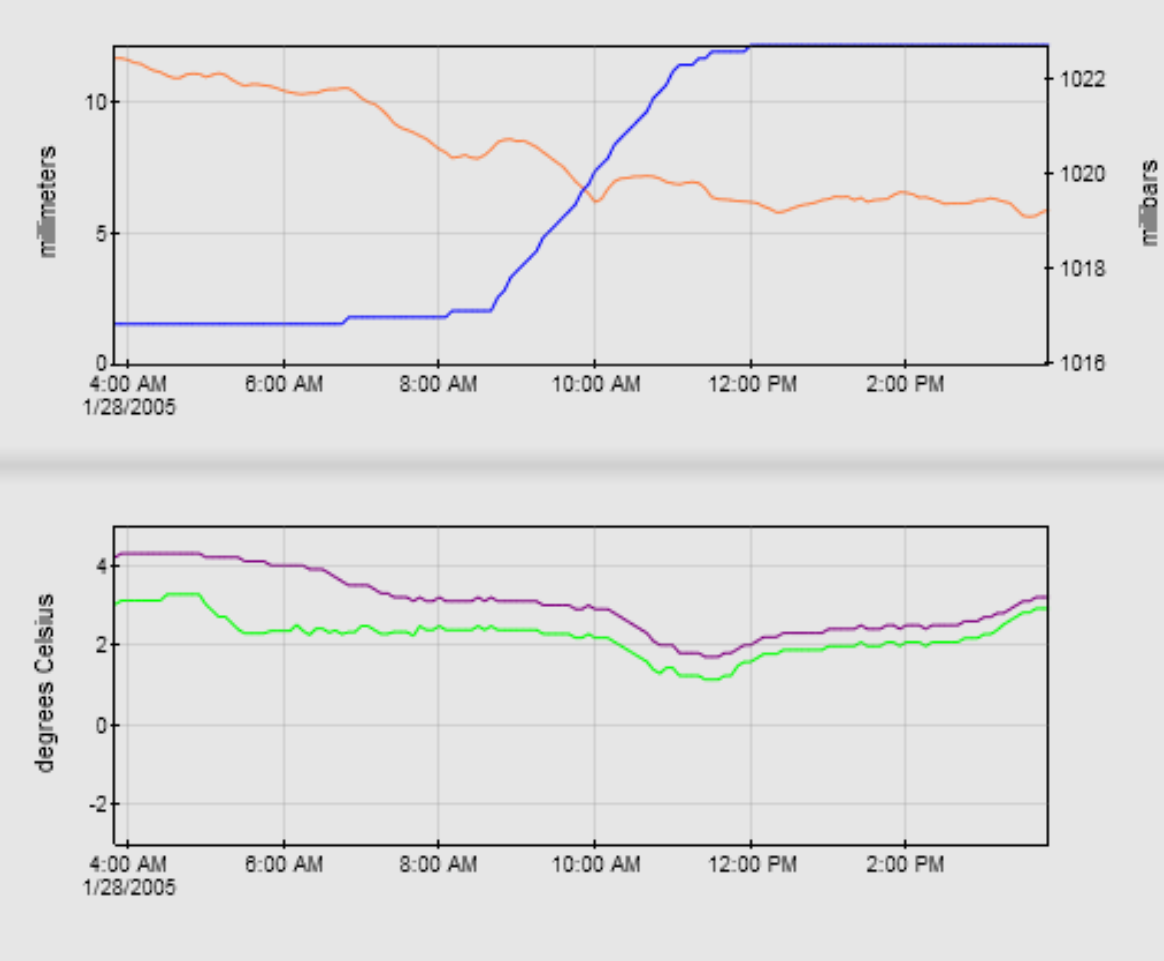

Figure 8c. As in 8a, but at TIPT.

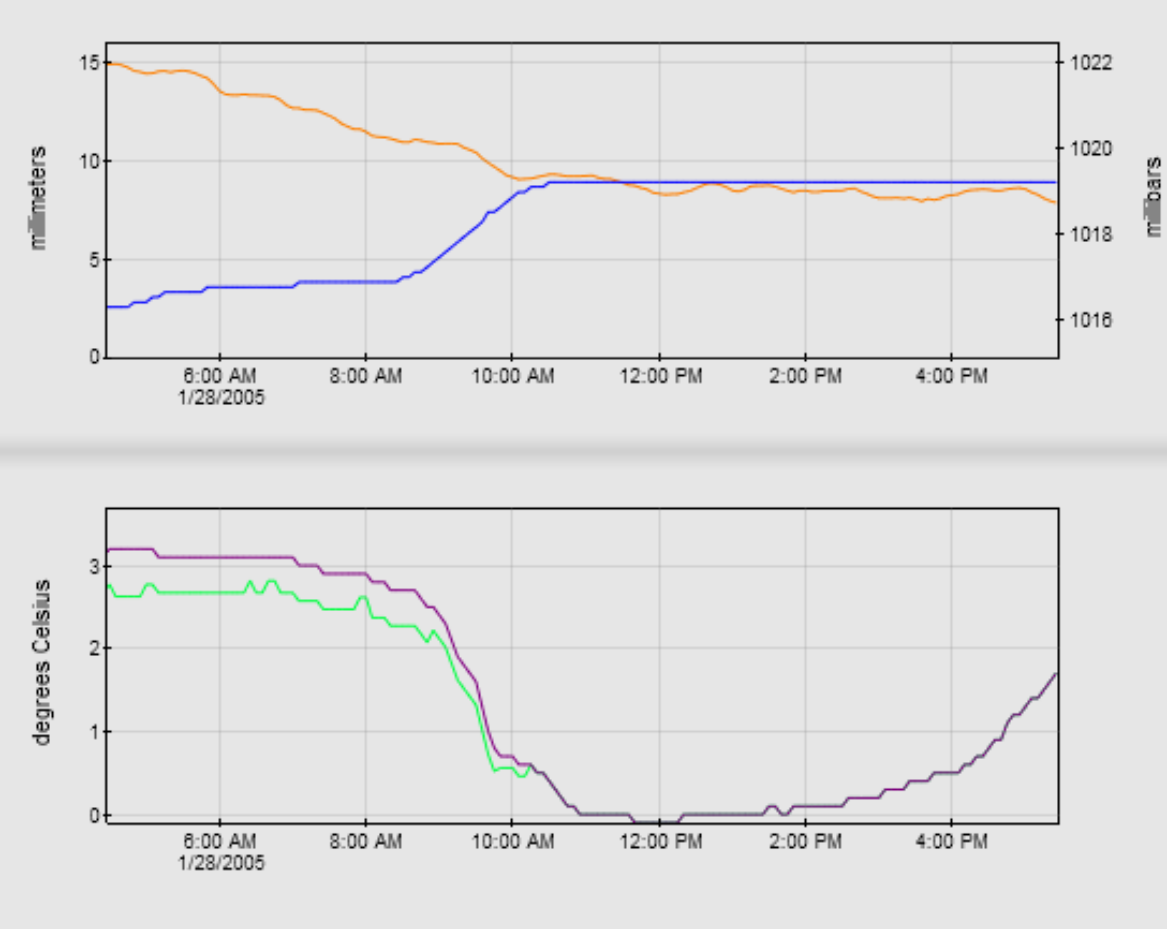

Figure 8d. As in 8a, but at MANG.

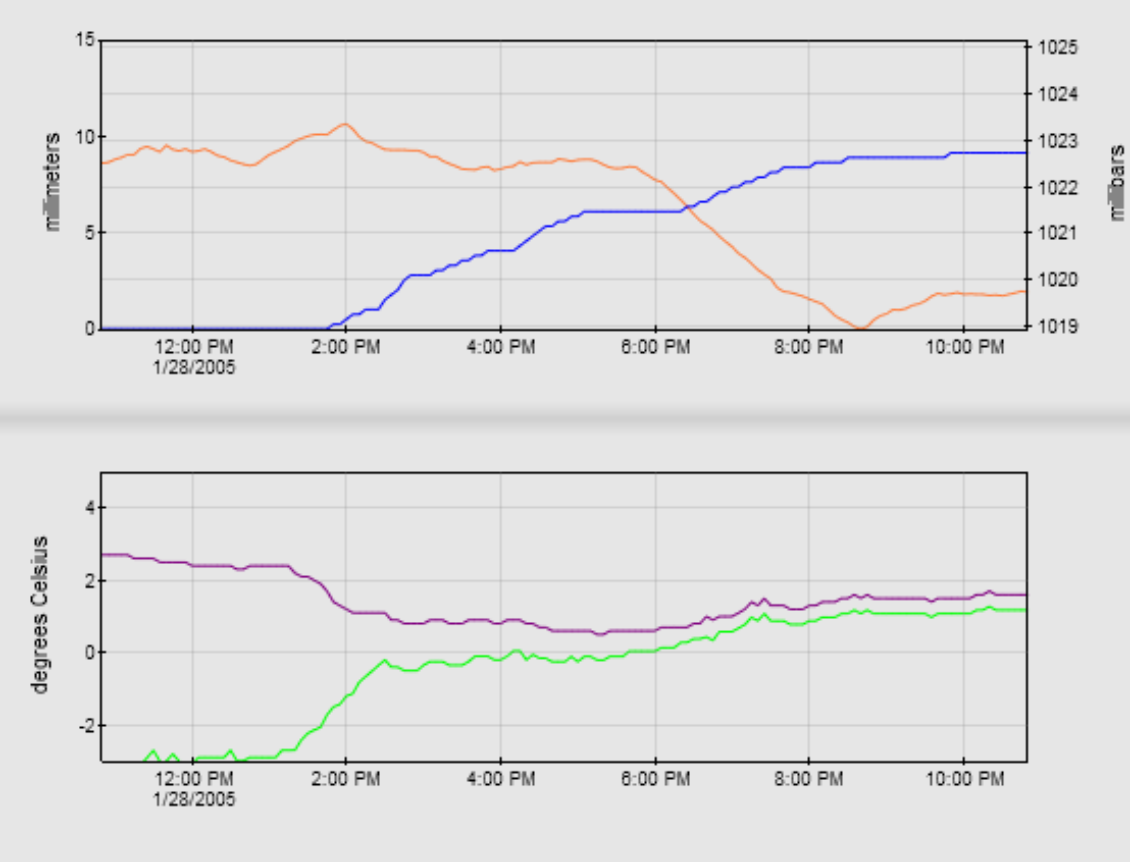

Figure 8e. As in 8a, but at OKEM.

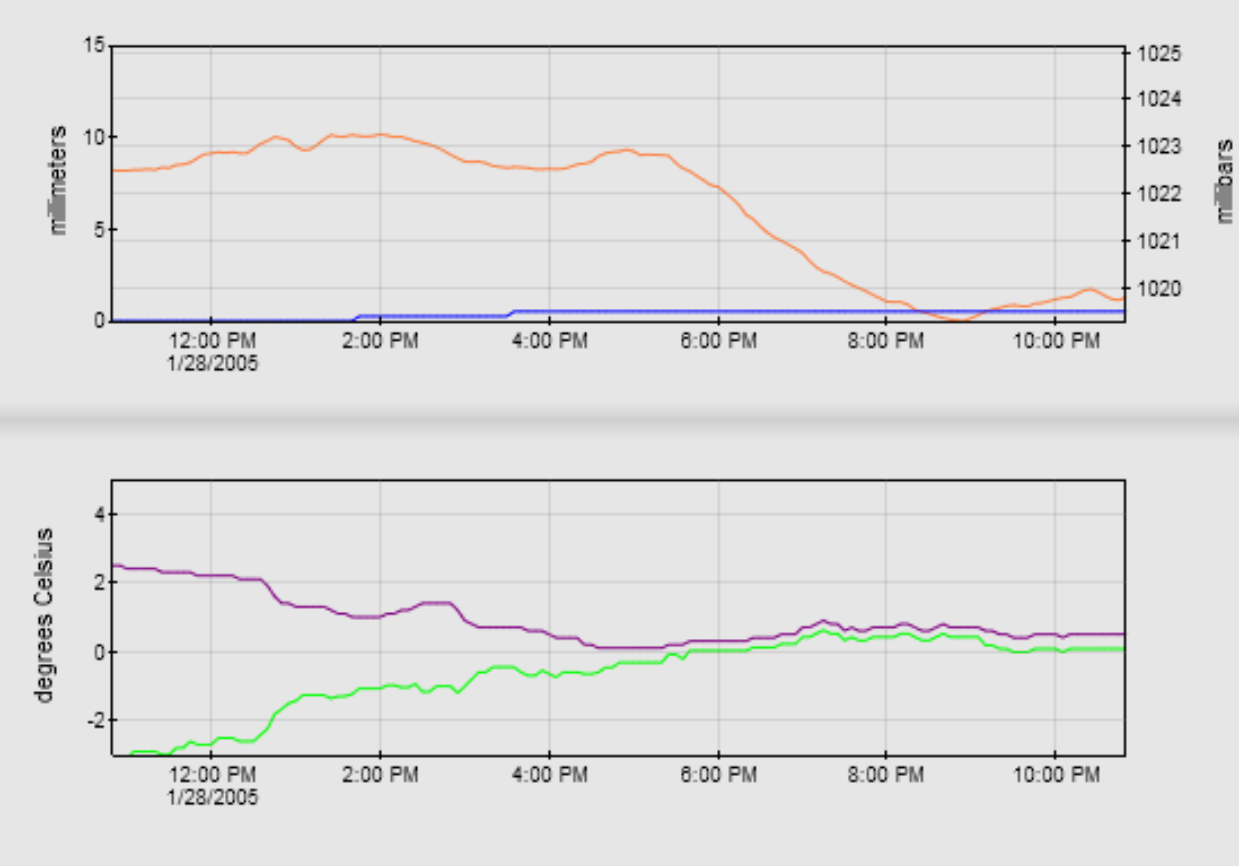

Figure 8f. As in 8a, but at OILT.

5. Evidence of melting-induced cold pools.

Figures 9a through 9c show maps of radar base reflectivities from KFDR, contoured pressure, gridded winds, mesonet temperature observations and mesonet side IDs at 0840 UTC, 1010 UTC, and 1030 UTC 28 January. Figure 9d shows surface divergence, calculated from the mesonet wind data, at 1015 UTC. A particularly intense bright band tracks eastward from Hollis (HOLL) to Altus (ALTU) and Tipton (TIPT) between 0830 UTC and 1030 UTC (figures 9a-9c) 28 January. In all the time series from western Oklahoma (figures 8a through 8d), the general pressure trend is falling pressures. This pressure trend is due to the eastward movement of the synoptic-scale surface trough located west of Oklahoma (figure 3d). However, at HOLL, ALTU, and TIPT (figures 8a-8c); the pressures rise for approximately a half hour as or just before the most intense bright banding reaches each respective station. At HOLL, the pressure begins rising

a few minutes before 0800 UTC and the highest base reflectivities (greater than 45dBZ) reach the station at 0840 UTC (figures 8a and 9a). With the exception of a small (0.2 degC) rise in temperature and dew point around 0900 UTC, the temperatures and dew points at HOLL drop off sharply after 0820 UTC (figure 8a). At ALTU, the pressure begins rising at 1000 UTC and the highest base reflectivities reach the station at 1010 UTC (figures 8b and 9b). The temperature and dew point at ALTU drops off sharply after 1030 UTC following the small (approximately 0.5hpa) rise in pressure (figure 8b). At TIPT, the pressure begins to rise at 1000 UTC and the highest reflectivities reach the station at 1030 UTC (figures 8c and 9c). The temperature and dew point at TIPT drop relatively sharply between 1000 UTC and 1100 UTC (figure 8c). The pressure and temperature tendencies at HOLL, ALTU, and TIPT are similar to pressure and temperature time series associated with the passage of convective cold pools (figure 1, Engerer et al 2008). At each station the sharpest drop in dew point and temperature occurs at the same time or within an hour after the pressure begins rising. Rises in pressure at the same time as or just before drops in temperature and dew point are consistent with the convective storm observations from Goff (1976). These signs of cold-pool outflow were associated with the passage of an area of particularly intense (greater than 45dBZ) bright-band reflectivities, suggesting that cooling from melting caused a downdraft where the most melting was occurring.

If a weak cold-pool downdraft did move across extreme southwestern Oklahoma between 9000 UTC and 1030 UTC, the one would expect divergent surface winds associated with the surface outflow in that region during the same time period. However, the gridded mesonet winds only show southeast winds without any indication of a wind shift near the highest bright-band reflectivities (figures 9a-9c). Similarly, figure 10a shows almost zero divergence near Tipton/Altus at 1015 UTC. The divergent winds from convective cold-pool outflow might not be located in the same place as the highest pressures (Vescio and Johnson, 1992). Because the pressure perturbation associated the bright band moved eastward while the surface air parcels moved northwestward, it might be more reasonable to expect divergence to the west of the highest perturbation pressures (Vescio and Johnson 1992). But there does not appear to be any divergence signature anywhere near the TIPT/ALTU stations at 1015 UTC- the surface divergence is nearly zero or negative throughout southwestern Oklahoma. The pressure and reflectivity tendencies at HOLL, ALTU, and TIPT between 0830 UTC and 1030 UTC suggest passage of a weak cold-pool, but the lack of a divergence signature suggests that no such downdraft existed.

Another possible cold-pool circulation was observed above the surface in radar radial velocity images. Figures 10a and 10b are images of level II base reflectivity and base radial velocity from KFDR at 1156 UTC, 28 January 2005. Figures 10c and 10d show reflectivity and velocity cross sections from KFDR at 1156 UTC, running from southwest (left) to northeast(right); the line in figures 10a and 10b indicate where the cross sections were taken. Figure 10e displays divergence, calculated from mesonet winds, at 1155 UTC. A strip of outbound velocities runs from northwest to southeast to the east of KFDR (figure 10b). The velocity pattern indicates convergence along the northeast edge of the strip of outbound velocities as well as divergence along the southwest edge of the strip. A line of bright-band reflectivities (greater than 40dbz) southeast of KFDR (figure 10a) is located in the area where the radial velocity image indicates divergence. The co-location of bright-band reflectivities and lower-level divergence suggests that a local downdraft was located in a region where the most melting was occurring. Figure 10d also suggests the presence of a downdraft- most outbound velocities are confined to levels above approximately 5000ft except within the strip of outbound

base velocities, suggesting that winds from the mid-levels were mixed down to the lower levels in a downdraft. This possible downdraft is located where a bright band indicates that the most melting is occurring, suggesting that a downdraft may have been caused by the cooling due to melting. The surface divergence (figure 10e) image does not reveal any areas of divergence corresponding to where the radar velocity image indicated divergence/convergence. However, in the area where the strip of divergent velocities southeast of KFDR aligns with the bright band reflectivities (figures 10a and 10b), the elevation of the 0.5 degree (the angle for base reflectivity and velocity) beam is between 2000ft and 6000ft above the level of the KFDR radar. The level II radar data shows signs of a downdraft from mid-to lower levels in an area southeast of KFDR. It is possible that such a downdraft existed but did not reach the surface- explaining the lack of a surface divergence signature.

Many other bright bands showed up in western Oklahoma between 09Z and 13Z 28 January, and none of them were associated with similar radar wind signatures to the one described above; which might mean that melting was not the only process responsible for the wind feature noted at 1156 UTC. This strip of low-level divergence might have instead been due to a convective downdraft. The 12Z OUN sounding shows that the mid-level lapse rate is nearly moist-adiabatic above the 850-750mb warm nose. Only a couple degrees Celsius difference in this profile would be required for conditional instability, and such a difference might have existed in southwest Oklahoma.

Based on the descriptions of convective cold pools (Engerer et al 2008; Wakimoto 1982), a cold pool outflow would be characterized by a sharp drop in both temperature and dew point coinciding with or following a positive perturbation in pressure and an area of positive divergence near the positive pressure perturbations (Vescio et al 1992). The bright band passing from HOLL to ALTU to TIPT had a pressure perturbation associated with it, but no corresponding region of divergence. The divergence signature noted in the radar velocity image at 1156 UTC 28 January (figures 10a and 10b) was not associated with any surface divergence signature, and time series from stations near the radar feature (not shown) did not reveal any consistent pattern of positive pressure perturbations co-located with the radial velocity feature. One area of divergent low-level winds was found in the same area as a bright band (figures 10a and 10b), but this wind feature may not have been caused solely by melting. So, both the pressure tendencies at HOLL, ALTU, and TIPT and the velocity feature east of KFDR cannot alone be interpreted as decisive indications of melting-induced cold-pool circulations. At most, both of the possible cold-pool features described provides some limited evidence of melting-driven downdrafts.

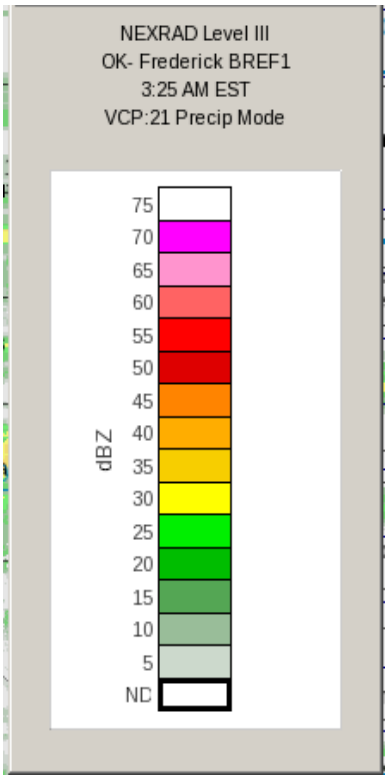

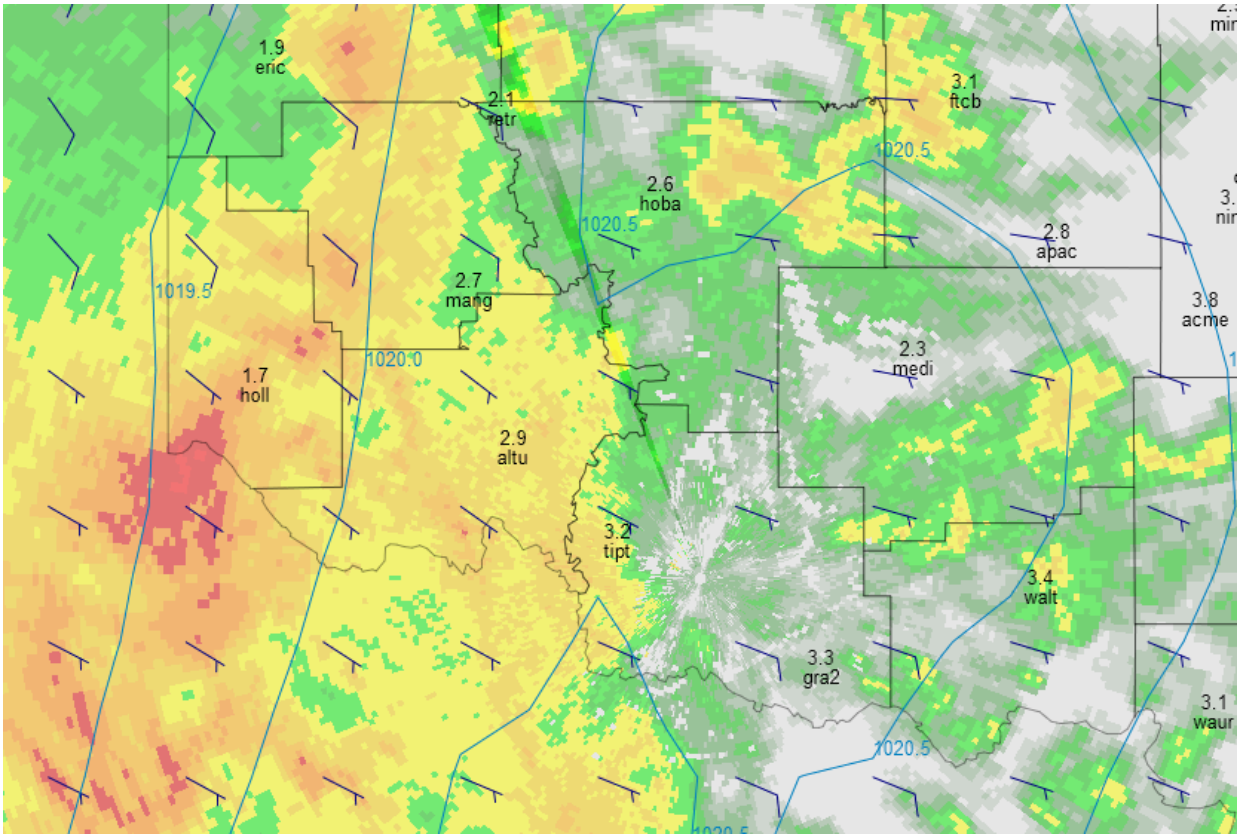

Figure 9a. KFDR base reflectivity, mesonet gridded winds (barbs), mesonet gridded sea-level pressure (blue contours), mesonet temperature observations and station IDs at 0840 UTC 28 January 2005. A legend for the reflectivity colors is above the figure. Temperature is in degrees Celsius, pressures are in hPa, wind is in knots.

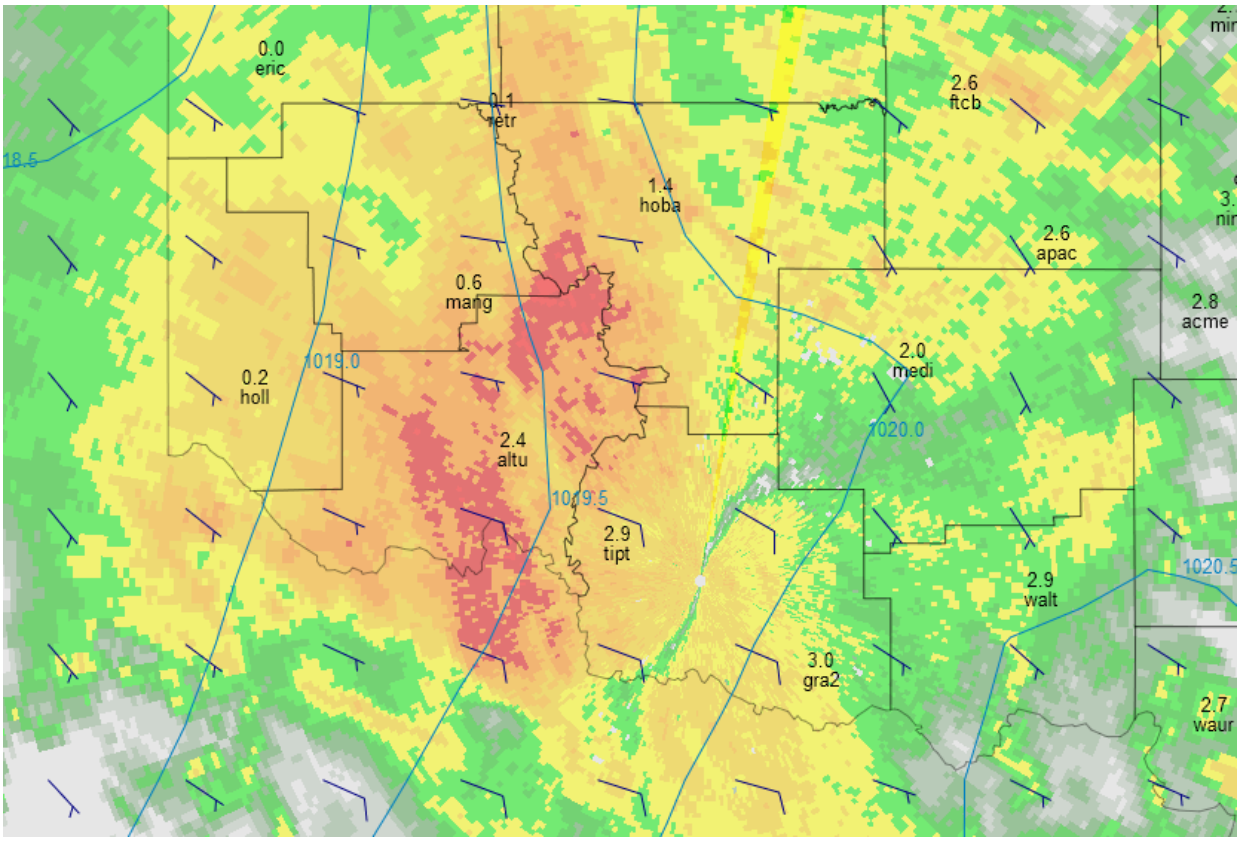

Figure 9b. As in 9a, but at 1010 UTC 28 January 2005.

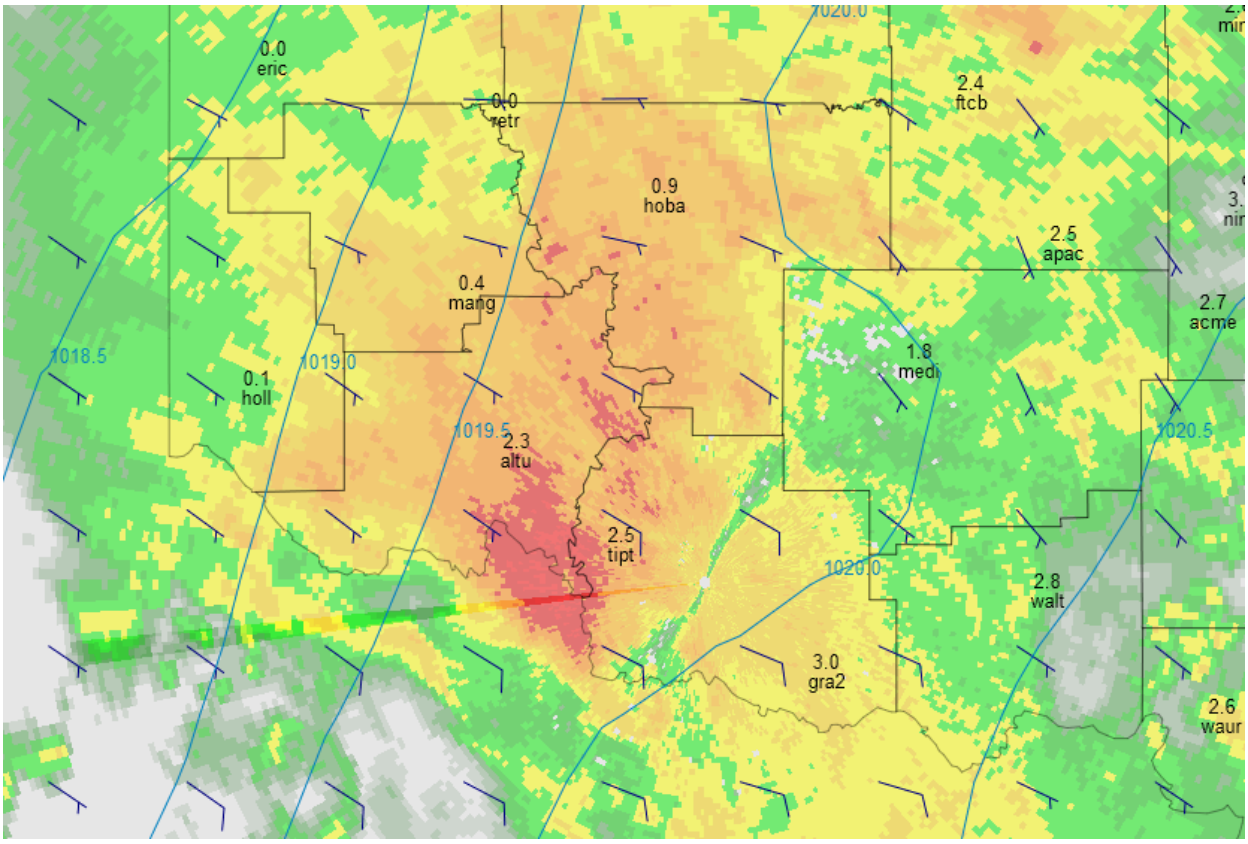

Figure 9c. As in 9a, but at 1030 UTC 28 January 2005. Note that the 1019.5hPa contour shifts westward between 1015 UTC (figure 9b) and 1030 UTC (above)- probably because of the rising pressures at ALTU and TIPT.

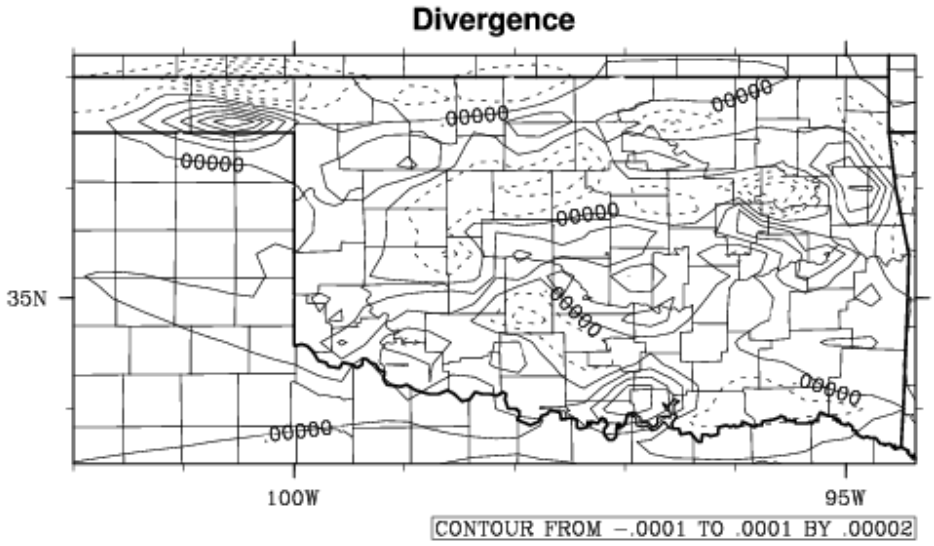

Figure 9d. Surface divergence (s^-1) at 1015 UTC 28 January 2005. Calculated from mesonet winds.

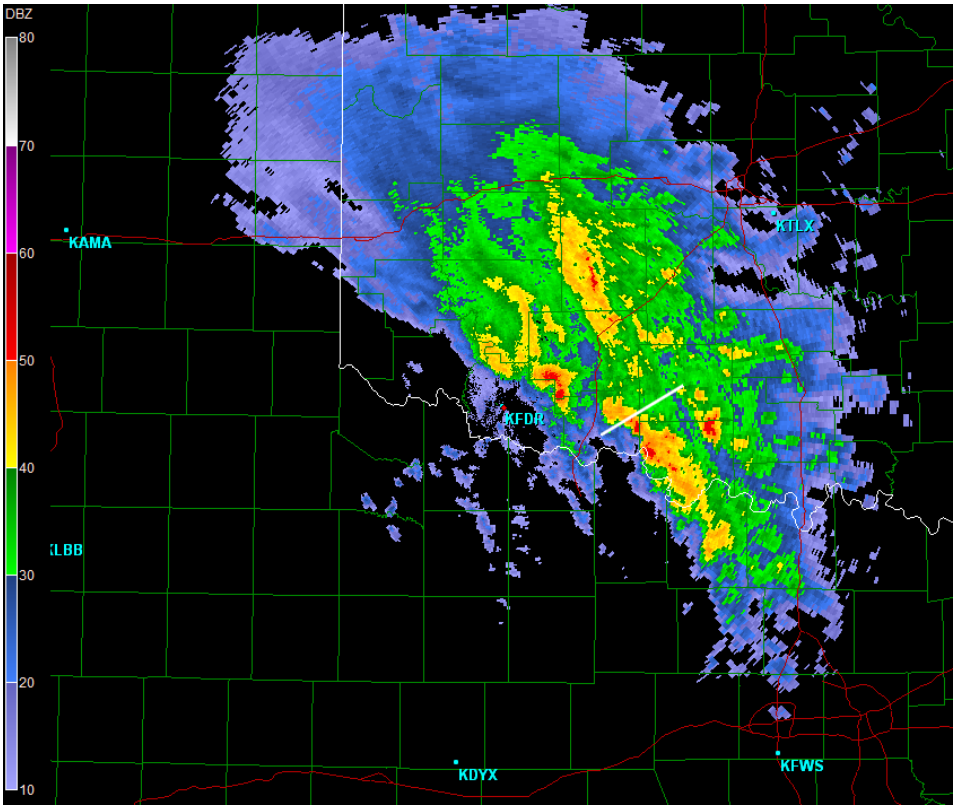

Figure 10a. KFDR base reflectivity at 1156 UTC 28 January 2005.

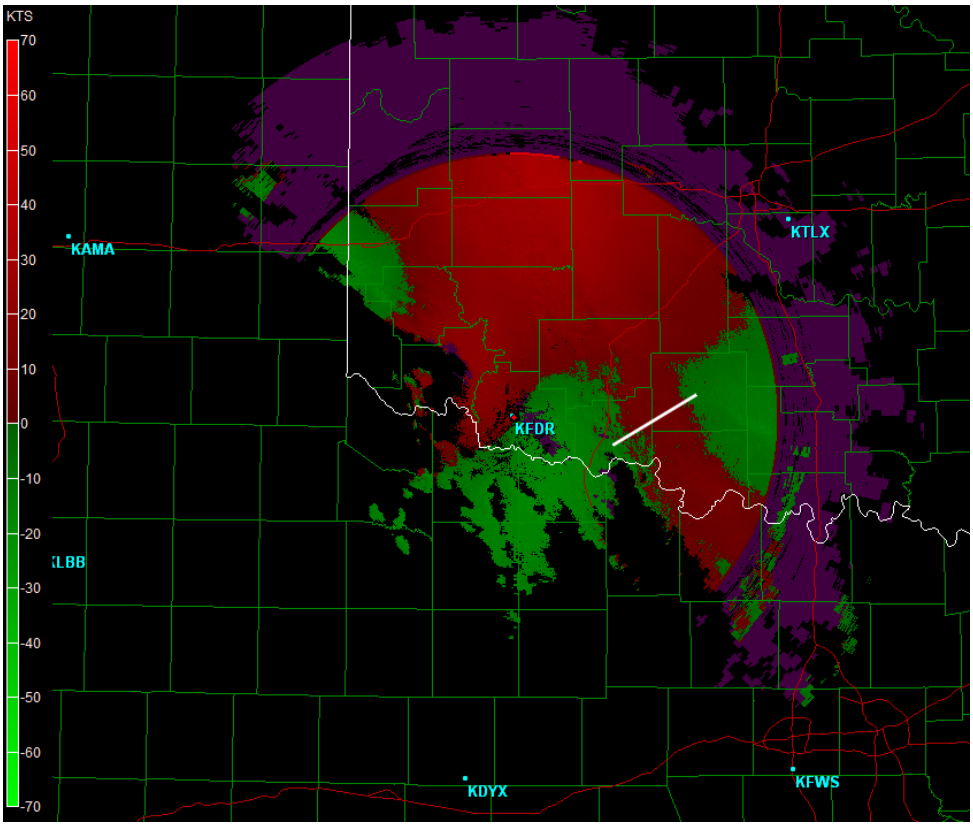

Figure 10b. KFDR base radial velocity at 1156 UTC 28 January 2005.

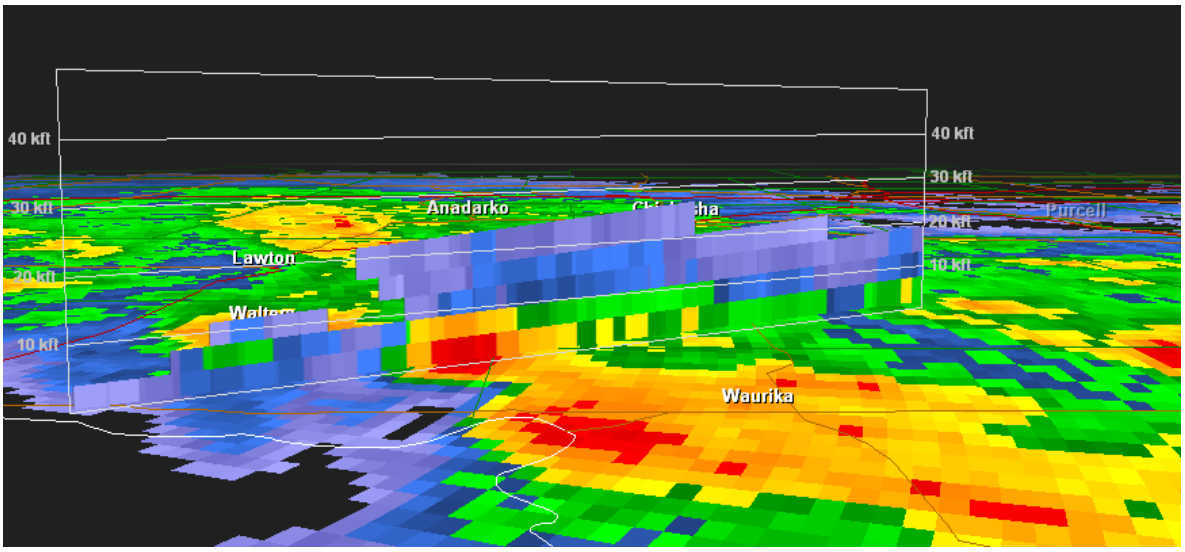

Figure 10c. KFDR reflectivity cross-section at 1156 UTC 28 January 2005.

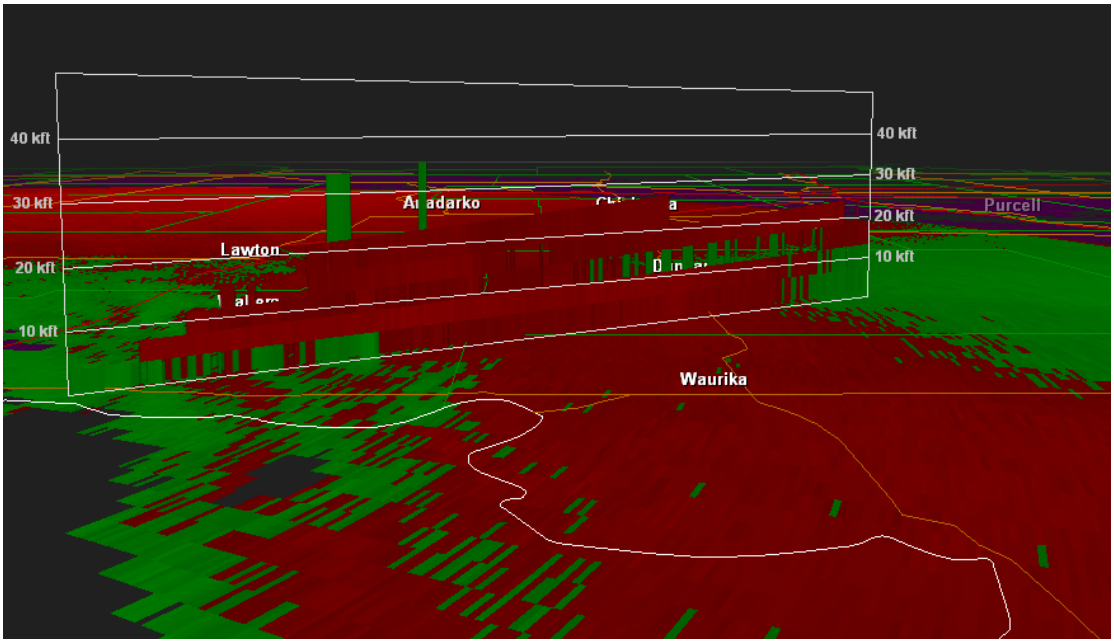

Figure 10d. KFDR velocity cross-section at 1156 UTC 28 January 2005.

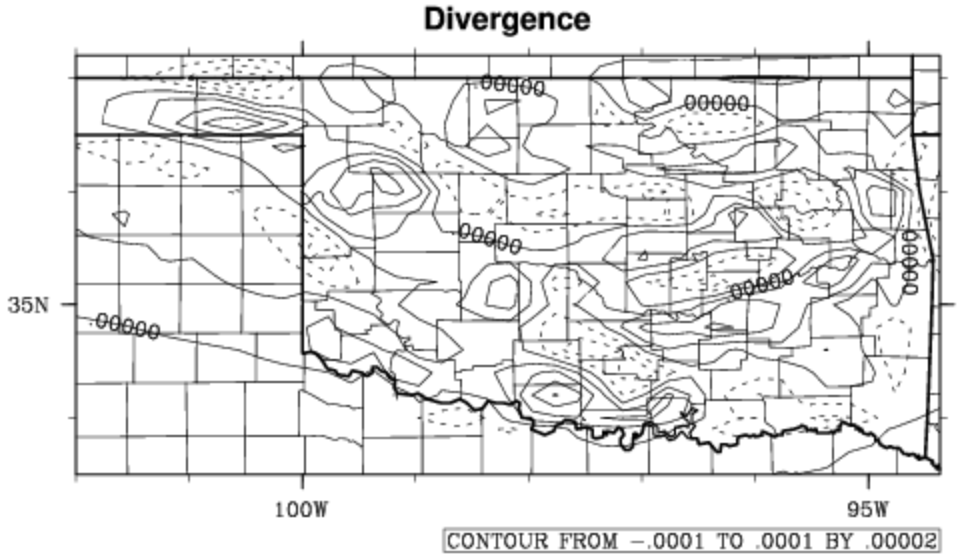

Figure 10e. Surface divergence at 1155 UTC 28 January 2005. Calculated from mesonet winds.

6. Summary and Conclusions.

A rain and snow event affected the state of Oklahoma on 28 January 2005. The mesoscale thermodynamic and dynamic characteristics of this event were inspected, with the intent of finding evidence of cold-pool circulations caused by melting.

A combination of sounding, wind profiler, radar, and surface mesonet data together showed that melting caused surface cooling in western Oklahoma, and evaporation caused surface cooling in eastern and central Oklahoma. The same data also suggest that melting was responsible for the elimination of a low-level warm layer in western Oklahoma.

Using Oklahoma Mesonet data and radar data from Frederick Air Force Base, conditions in southwest Oklahoma were studied in detail to look for possible indications of melting-driven cold-pool outflows. Some limited and therefore inconclusive evidence for such cold-pools was found. In one case, pressure rises were observed to occur at three stations as an intense bright band approached those stations. In the other case, a bright band occurred in the same area that a radar radial velocity image indicated low-level divergence.

It was a mistake on the part of the author to select a case that was characterized by two layers of above-freezing air at the onset of the precipitation. Downdrafts may have been generated by melting precipitation in both warm layers, but the downdrafts might have interacted in such a way as to cancel each other out, and downdrafts from the melting in a lower-level warm layer might have complicated the pressure field at the surface. Future investigations of the dynamical impacts of melting might start by selecting a case where only one layer of above-freezing air exists. With such a case, the relationship between cooling from melting and the surface pressure field might become clearer.

Acknowledgments

This research was completed for a two-semester Undergraduate Research course at SUNY Albany. Professor Ryan Torn advised the research: I would like to thank Ryan Torn for helping to plan the research, discussing and commenting on the findings, and reviewing earlier versions of this manuscript. I wish to thank Professor Lance Bosart for his commentary on the early findings of this project, and Mary Haley (NCAR) and Mathew Janiga (SUNY Albany) for their help debugging NCL scripts. Kevin Tyle downloaded the WeatherScope software onto each of the SUNY Albany maproom computers and helped the author debug Bash scripts. The Oklahoma Climate Survey staff provided helpful instructions on how to use the WeatherScope software.

References

Bosart, L.F and F Sanders, 1991: An Early-Season Coastal Storm: Conceptual Success and Model Failure. *Mon. Wea. Rev.*, **119**, 2831–2851.

Brock, F.V; K.C Crawford; R.L Elliot; G.W Cuperus; S.J Stadler; H.L Johnson and M.D Eilts, 1995: The Oklahoma Mesonet: A technical overview. *J. Atmos. Oceanic Technol.*, **12**, 5-19.

Chen, S and W.R Cotton, 1988: The Sensitivity of a Simulated Extratropical Mesoscale Convective System to Longwave Radiation and Ice-Phase Microphysics. *J. Atmos. Sci.*, **45**, 3897–3910.

Engerer, N.A; D.J Stensrud and M.C Coniglio, 2008: Surface Characteristics of Observed Cold Pools. *Mon. Wea. Rev.*, **136**, 4839–4849.

Craig Goff, R, 1976: Vertical Structure of Thunderstorm Outflows. *Mon. Wea. Rev.*, **104**, 1429–1440.

Grim, J.A; G.M McFarquhar; R.M Rauber; A.M Smith and B.F Jewett, 2009: Microphysical and Thermodynamic Structure and Evolution of the Trailing Stratiform Regions of Mesoscale Convective Systems during BAMEX. Part II: Column Model Simulations. *Mon. Wea. Rev.*, **137**, 1186–1205.

Heffernan, E and J Marwitz, 1996: The Front Range Blizzard of 1990. Part II: Melting Effects in a Convective Band. *Mon. Wea. Rev.*, **124**, 2469–2482.

Heymsfield, G.M, 1979: Doppler Radar Study of a Warm Frontal Region. *J. Atmos. Sci.*, **36**, 2093–2107.

Jorgensen, D.P; M.A LeMone and S.B Trier, 1997: Structure and Evolution of the 22 February 1993 TOGA COARE Squall Line: Aircraft Observations of Precipitation, Circulation, and Surface Energy Fluxes. *J. Atmos. Sci.*, **54**, 1961–1985.

Kain, J.S; S.M Goss and M.E Baldwin, 2000: The Melting Effect as a Factor in Precipitation-Type Forecasting. *Wea. Forecasting*, **15**, 700–714.

Kim, D.K; K.R Knupp and C.R Williams, 2009: Airflow and Precipitation Properties within the Stratiform Region of Tropical Storm Gabrielle during Landfall. *Mon. Wea. Rev.*, **137**, 1954–1971.

Knupp, K.R, 1988: Downdrafts within High Plains Cumulonimbi. Part II: Dynamics and Thermodynamics. *J. Atmos. Sci.*, **45**, 3965–3982.

Lackmann, G.M; K Keeter; L.G Lee and M.B Ek, 2002: Model Representation of Freezing and Melting Precipitation: Implications for Winter Weather Forecasting. *Wea. Forecasting*, **17**, 1016–1033.

Leary, C.A and R.A Houze, 1979: Melting and Evaporation of Hydrometeors in Precipitation from the Anvil Clouds of Deep Tropical Convection. *J. Atmos. Sci.*, **36**, 669–679.

Lee, W.C, R.E Carbone and R.M Wakimoto, 1992: The Evolution and Structure of a "Bow-Echo–Microburst" Event. Part I: The Microburst. *Mon. Wea. Rev.*, **120**, 2188–2210.

Phillips, V. T. J; A Pokrovsky and A Khain, 2007: The Influence of Time-Dependent Melting on the Dynamics and Precipitation Production in Maritime and Continental Storm Clouds. *J. Atmos. Sci.*, **64**, 338–359.

Sanders, F and R.J Paine, 1975: The Structure and Thermodynamics of an Intense Mesoscale Convective Storm in Oklahoma. *J. Atmos. Sci.*, **32**, 1563–1579.

Stewart, R.E and P King, 1987: Rain–Snow Boundaries over Southern Ontario. *Mon. Wea. Rev.*, **115**, 1894–1907.

Szeto, K.K; C.A Lin and R.E Stewart, 1988: Mesoscale Circulations Forced by Melting Snow. Part I: Basic Simulations and Dynamics. *J. Atmos. Sci.*, **45**, 1629–1641.

-------, R.E Stewart and C.A Lin, 1988: Mesoscale Circulations Forced by Melting Snow. Part II: Application to Meteorological Features. *J. Atmos. Sci.*, **45**, 1642–1650.

------- and R. E Stewart, 1997: Effects of Melting on Frontogenesis. *J. Atmos. Sci.*, **54**, 689–702.

Szyrmer, W and I Zawadzki, 1999: Modeling of the Melting Layer. Part I: Dynamics and Microphysics. *J. Atmos. Sci.*, **56**, 3573–3592.

Vescio, M.D and R.H Johnson, 1992: The Surface-Wind Response to Transient Mesoscale Pressure Fields Associated with Squall Lines. *Mon. Wea. Rev,* **120**, 1837-1850.

Wakimoto, R.M, 1982: The Life Cycle of Thunderstorm Gust Fronts as Viewed with Doppler Radar and Rawinsonde Data. *Mon. Wea. Rev.*, **110**, 1060–1082.

Wei, Y and J Marwitz, 1996: The Front Range Blizzard of 1990. Part III: Numerical Simulations of Melting Effects. *Mon. Wea. Rev.*, **124**, 2483–2496.

Yang, M.H and R.A Houze, 1995: Sensitivity of Squall-Line Rear Inflow to Ice Microphysics and Environmental Humidity. *Mon. Wea. Rev.*, **123**, 3175–3193.

Martin, J.E, 2006: The Quasi-Geostrophic System of Equations. *Mid-Latitude Atmospheric Dynamics: A First Course,* John Wiley & Sons Inc., 139.

Baumgardt, D, 1999: Wintertime Cloud Microphysics Review, cited 2011. [Availabe online at http://www.crh.noaa.gov/arx/micro/micrope.php]

Steigerwaldt, H. 1998: The role of cynamic cooling in the snowstorm on the eastern highland rim and Cumberland Plateau of Tennesee, cited 2011. [Available online at http://www.srh.noaa.gov/topics/attach/html/ssd98-10.htm]

NCAR Image Archive, cited 2011. [Available online at http://www.mmm.ucar.edu/imagearchive/]

NOMADS Model Database, cited 2011. [Available online at http://nomads.ncdc.noaa.gov/]

Norman Oklahoma National Weather Service Forecast Office Preliminary Storm Reports, cited 2011. [Available online at http://www.srh.noaa.gov/oun/?n=stormdata]

Storm Prediction Center Surface and Upper-Air Maps, cited 2011. [Available online at http://www.spc.nssl.noaa.gov/obswx/maps/]

University of Wyoming Soundings Page. [Available online at http://weather.uwyo.edu/upperair/sounding.html]

Scott-Gibson, M. GR2Analyst. Gibson Ridge Software, LLC

Oklahoma Climate Survey. WeatherScope (software) [Available online at www.mesonet.org]